Journal of Hazardous Materials 489 (2025) 137696

Contents lists available at ScienceDirect

Journal of Hazardous Materials

journal homepage: www.elsevier.com/locate/jhazmat

Assessment of aerobic-anoxic biotrickling filtration for the desulfurization of high-strength H_2S streams from sugarcane vinasse fermentation

André Do Vale Borges [a,b], Márcia Helena Rissato Zamariolli Damianovic [b], Raúl Muñoz Torre [a,c,*]

[a] Institute of Sustainable Processes, Dr. Mergelina, s/n, Valladolid 47011, Spain
[b] Biological Processes Laboratory (LPB), São Carlos School of Engineering (EESC), University of São Paulo (USP), Av. João Dagnone, 1100, Santa Angelina, São Carlos, São Paulo 13563-120, Brazil
[c] Department of Chemical Engineering and Environmental Technology, School of Industrial Engineering, University of Valladolid, Dr. Mergelina, s/n, Valladolid 47011, Spain

HIGHLIGHTS

- Novel BTF design optimized for H2S-rich biogas from vinasse fermentation.
- Complete H2S removal achieved at gas contact times as low as 4 min.
- Low surface area (490 m3 m-2) media outperformed micro rings, avoiding clogging.
- Maximum elimination capacity of 160 gS-H2S m-3 h-1 with stable performance.
- Hybrid aerobic-anoxic systems effectively balanced sulfur oxidation and stability.

GRAPHICAL ABSTRACT

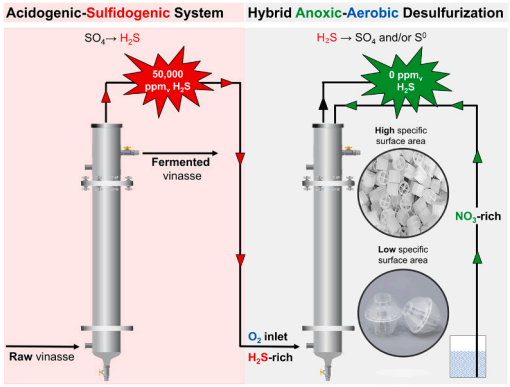

ARTICLE INFO

Keywords:
Acidogenic fermentation
Autotrophic denitrification
Biotrickling filter
Hydrogen sulfide
Hybrid aerobic-anoxic trickling systems

ABSTRACT

The increasing demand for renewable energy has heightened interest in biogas production from agro-industrial residues, such as sugarcane vinasse—a byproduct of ethanol production. During vinasse fermentation, sulfate reduction generates biogas with high hydrogen sulfide (H_2S) concentrations, reaching up to 50,000 ppm_v. This study assessed the performance of two bench-scale biotrickling filters (BTFs) treating synthetic sulfide-rich acidogenic off-gas (7000 ppm_v) from mesophilic sugarcane vinasse fermentation. The systems were packed with materials of high (950 m^2 m^{-3}, BTF_H) and low (460 m^2 m^{-3}, BTF_L) specific surface areas and inoculated with sulfur-oxidizing bacteria (SOB). Operational conditions included decreasing empty bed residence times (EBRTs) of 9, 6, and 4 min and nitrate-to-sulfur ratios of 0.1, 0.3, and 0.5, respectively. Both BTFs achieved complete H_2S removal at the shortest EBRT, with elimination capacities (ECs) exceeding 140 g S-H_2S m^{-3} h^{-1}. However, BTF_H exhibited reduced EC at higher H_2S loads due to elemental sulfur (S^0) accumulation, resulting in clogging, pH instability, and diminished denitrification activity. Despite these challenges, the system demonstrated resilience by restoring nitrate reduction and H_2S oxidation. This study underscores the efficacy of hybrid

* Corresponding author at: Institute of Sustainable Processes, Dr. Mergelina, s/n, Valladolid 47011, Spain.
E-mail addresses: mutora@iq.uva.es, mutoraul@gmail.com (R.M. Torre).

https://doi.org/10.1016/j.jhazmat.2025.137696
Received 15 December 2024; Received in revised form 9 February 2025; Accepted 19 February 2025
Available online 20 February 2025

aerobic-anoxic BTFs for treating H_2S-rich biogas and highlights the critical role of packing material selection and nitrogen-to-sulfur ratio control for long-term operational stability.

1. Introduction

The increasing global demand for energy, driven by population growth and rising consumption, has significantly intensified fossil fuel use over recent decades. National and international legislative efforts have united countries in the pursuit of sustainable energy solutions that foster economic growth. Biogas has emerged as a globally recognized renewable energy source, offering both environmental and economic benefits. It is typically produced through anaerobic digestion (AD) of organic matter [1]. Agro-industrial by-products, such as wastewater from cassava [57,58], breweries [69], dairies [82], coffee grounds [25], slaughterhouses [48], and sugarcane crops [35], are especially suitable for AD to increase biogas production. In Brazil, biogas production primarily relies on sugarcane vinasse, a major by-product of the sugar-ethanol industry [10,11]. Biogas applications in AD biorefineries include electricity generation, heat production, and upgrading to biomethane for grid injection or use as transportation fuel [34]. Regardless of its application, biogas requires impurity removal to concentrate methane and prevent damage to energy valorization units [93].

Sugarcane vinasse contains sulfur compounds, mainly sulfate, which are reduced by sulfate-reducing bacteria (SRB) into sulfide [36]. Depending on the pH, sulfide is released as hydrogen sulfide (H_2S), a corrosive gas that damages metals, engines, pipelines, and concrete. H_2S also produces harmful sulfur oxides (SO_x) during combustion, posing risks to health and the environment [54,65]. The limiting H_2S concentration for biogas used in internal combustion engines should not exceed 300 ppm_v [45]. Two-phase AD systems (2nd-AD) separate acidogenesis and methanogenesis, minimizing competition for key substrates such acetate and hydrogen, generating partial alkalinity, and reducing the need for sodium-based chemical additives [12,79]. In this setup, sulfate reduction occurs during acidogenesis, preventing sulfate's inhibitory effects on methanogenic archaea (MA) [33]. Recent studies on sugarcane vinasse 2nd-AD have demonstrated 90–99 % sulfate reduction, producing sulfide-rich acidogenic off-gas with up to 10 % H_2S, primarily composed of CO_2 (70–99 %) and H_2 (1–30 %) [12,33,71]. Despite this, the sustainable management of sulfide-rich acidogenic off-gas remains unexplored.

In-situ and *ex-situ* technologies for sulfide removal from biogas—collectively termed desulfurization methods—are well-documented [17,2,42,73]. *In-situ* approaches involve micro-aeration or iron salt dosing, while *ex-situ* methods use separate units for physicochemical or biological processes [20,7]. Although physicochemical systems dominate the market, biological desulfurization offers advantages, including lower operating costs, reduced chemical use, lower energy consumption, and non-hazardous by-products [22,54,73].

Chemotrophic processes can be engineered as biotrickling filters (BTFs), which exhibit high H_2S tolerance (up to 12,000 ppm_v H_2S), offer compact designs, and simplified operation [31,45]. These systems use packed beds inoculated with sulfide-oxidizing bacteria (SOB) to oxidize H_2S to elemental sulfur (S^0) or sulfate under aerobic or anoxic conditions [65]. S^0, preferred for its stability, reusability, and lower oxygen demand, can accumulate due to oxygen mass transfer limitations at high H_2S loads, causing operational issues [60,90]. While the optimization of operating parameters in aerobic systems, including the O_2 to H_2S ratio, trickling liquid velocity (TLV), and in anoxic systems, the nitrate-to-sulfur ratio, has been extensively investigated, research on integrated aerobic-anoxic systems aimed at achieving cost-effectiveness and long-term sustainable performance in biotrickling filters (BTFs) under high H_2S load conditions remains limited. Efficient sulfur management also depends on packing material selection [55,81]. Macroporous material such as activated carbon enhance microbial attachment [18,27], while microporous materials such as polyurethane foam improve gas distribution and reduce pressure drops [31,37,67,75]. Hydrophilic and chemically stable materials, such as polyethylene, maintain moisture and resist acidic conditions [56,68]. Packing structure influences clogging risk, with small pores trapping S^0 and open structures promoting washout [8,66]. Operational parameters, including oxygen availability, liquid recirculation rate, and empty bed residence time (EBRT), significantly impact performance [100,50,77]. More recently, studies have reported the role of heavy metals (e.g., iron) in enhancing contaminant degradation [88].

To date, biological desulfurization has primarily targeted raw biogas from single-stage AD systems (methanogenic reactors) to meet biomethane standards or engine manufacturer H_2S specifications [59,83,87]. Raw biogas typically comprises CH_4 (40 – 75 %), CO_2 (15 – 60 %), and H_2S (< 2 %), depending on the feedstock and AD process. However, no studies have investigated BTFs for desulfurizing high-strength H_2S streams (up to 10 %) from acidogenic reactors [12,33,71,80]. This gap in research highlights the need for tailored solutions to manage acidogenic-off gas desulfurization under challenging conditions characteristic of acidogenic effluent treatment.

This study fills this critical gap by evaluating the performance of two-bench scale BTFs under mesophilic conditions, simulating high-strength H_2S emissions from sugarcane vinasse fermentation at several EBRTs. The systems were equipped with two packing materials, each featuring different specific surface areas, randomly distributed within the bed. The aim was to evaluate their impact on H_2S removal efficiency and by-products accumulation. A deeper understanding of biological desulfurization processes in high H_2S streams is essential for minimizing sulfur emissions, overcoming operational challenges in sugarcane biorefineries, and recovering biomass and nutrients.

2. Material and methods

2.1. Inocula and mineral salt medium

A 1:1 v/v mixture of activated sludge (~ 8.0 g-VSS L^{-1}) obtained from Valladolid Wastewater Treatment Plant (WWTP), operated in a denitrification-nitrification configuration, and algal-bacterial biomass (~ 4.6 g-VSS L^{-1}) was used to inoculate both BTF systems. The aerobic algal-bacterial communities, previously adapted to a continuous flow of 5000 ppm_v H_2S, were sampled from a 180 L pilot high-rate algal pond treating diluted centrate at the Institute of Sustainable Processes (University of Valladolid, Spain).

The liquid trickling solution consisted of a Mineral Salt Medium (MSM) prepared with distilled water and micronutrients, as described by Pascual et al. [70]. The MSM was composed of (g L^{-1}): potassium dihydrogen phosphate (0.7), dipotassium hydrogen phosphate trihydrate (0.917), potassium nitrate (3.0), sodium chloride (0.2), magnesium sulfate heptahydrate (0.345), calcium chloride dihydrate (0.026), and 2 mL L^{-1} of a micronutrient solution composed of (g L^{-1}): EDTA (0.5), iron (II) sulfate heptahydrate (0.2), zinc sulfate heptahydrate (0.01), manganese dichloride tetrahydrate (0.003), boric acid (0.003), cobalt (II) chloride hexahydrate (0.02), copper (II) chloride dihydrate (0.001), nickel (II) chloride hexahydrate (0.002), and sodium molybdate dihydrate (0.003) (Sigma Aldrich, San Luis, USA). No supplementation of inorganic carbon (IC) in the form of HCO_3^- was carried out.

2.2. Experimental set up

Two laboratory-scale BTF systems, each consisting of a cylindrical acrylic column with a diameter of 8.4 cm and a height of 26.5 cm, were

operated independently and continuously under mesophilic conditions (27.0 ± 1.0 °C) for more than 100 days. The packed bed columns were interconnected to a 1 L stirred tank reactor provided with automatic pH control (Fig. 1). The systems, with packed-bed volumes of 1.0 L, were used to treat a synthetic reference biogas [12] with the following composition: CO_2 (82 ± 8 %), and H_2S (5 ± 3 %). The gas mixture after air dilution was composed of CO_2 (11.7 ± 0.9 %), O_2 (17.8 ± 0.2 %), N_2 (69.0 ± 0.8 %), and H_2S (0.7 ± 0.04 %). The H_2S gas stream (50, 000 ppm_v) was introduced into the mixing chamber using a peristaltic pump (Watson Marlow, United Kingdom, UK) from a 30 L gas sampling bag (Tedlar® PVF film) containing 22 % H_2S and 78 % N_2. A mass flow controller and a flow meter (Aalborg, New York, USA) were used to regulate the CO_2 stream from a pressurized gas cylinder (Abello Linde, Spain), while ambient air was pumped via an air compressor. The supplied O_2:H_2S ratio (v v^{-1}) was maintained at 24.0, as described elsewhere [32,62,64]. A sketch of the experimental setup is depicted in Fig. 1.

In the first BTF, referred to as BTF_H, the support material consisted of wheel-shaped polyethylene media (Kaldnes K1 Micro rings, Evolution Aqua, UK) with a specific surface area of 950 m^2 m^{-3} (7 mm diameter, 9 mm length). In the second BTF, referred to as BTF_L, a mixture of polyhedral plastic hollow balls designed for wastewater treatment (Latino, China) was used, which were characterized by a lower specific surface area of 460 m^2 m^{-3} (25 mm diameter, 25 mm height). Table 1 shows the main operating parameters set in both BTFs.

Both BTF_H and BTF_L were operated under countercurrent mode, with the biogas-air mixture entering at the bottom of the column at varying flowrates (Q) (159.7 – 359.49 L d^{-1}) at three different operating stages (Table 2). The systems were continuously irrigated from the top of the BTFs with the MSM via a peristaltic pump (Dinko Instruments, Barcelona, Spain) at a linear trickling liquid velocity (TLV) of 2 m h^{-1}, as described by Jia et al. [41]. The recycled MSM was renewed in a semi-continuous mode by replacing 100 mL (Stage I), 300 mL (Stage II),

Table 1
Operating parameters applied to BTF_H and BTF_L.

Parameters	Values
pH	7.0
Temperature	27.0 ± 1.0 °C
Electron donor(s)	H_2S
Electron acceptor(s)	O_2 and NO_3^-
MSM loading rate	0.2 L min^{-1}
Trickling liquid velocity (TLV)	2 m h^{-1}
O_2:H_2S	24.0
Packing material	Kaldnes K1 (BTF_H) and polyethylene hollow balls (BTF_L)
Packed bed volume	1.0 L
Type of operation	Counter current

Note: BTF_H – biotrickling filter with "high" specific surface area, BTF_L – biotrickling filter with "low" specific surface area.

Table 2
Operating stages applied to BTF_H and BTF_L.

Reactor	Days of operation	$Q_{BIOGAS*}$ (m^3 d^{-1})	$[H_2S]_{in}$ (gS-H_2S m^{-3})	LR (gS-H_2S m^{-3} h^{-1})	EBRT (min)
BTF_H	I (15 – 29)	0.16	8.7 ± 0.5	58.1 ± 3.4	9.0
	II (29 – 59)	0.24	9.8 ± 0.5	103.6 ± 5.7	6.0
	III (59 – 101)	0.36	9.7 ± 0.4	151.7 ± 8.9	4.0
BTF_L	I (15 – 40)	0.16	9.3 ± 0.8	61.8 ± 5.4	9.0
	II (40 – 77)	0.24	9.3 ± 0.6	92.6 ± 6.0	6.0
	III (77 – 112)	0.36	9.4 ± 0.4	141.2 ± 6.5	4.0

$[H_2S]_{in}$ – inlet H_2S concentration, LR – loading rate, EBRT – empty bed residence time. *After air dilution.

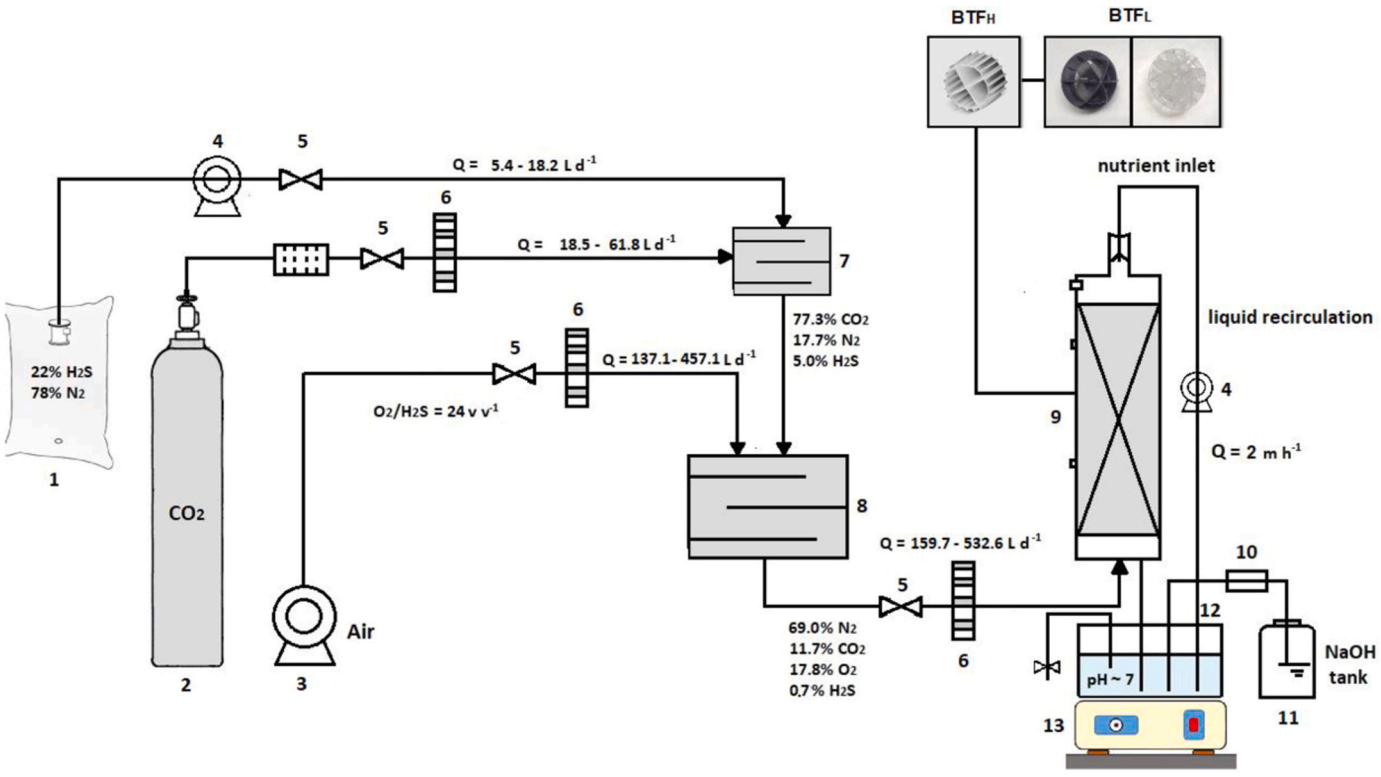

Fig. 1. Schematic view of the experimental set-up. (1) 30 L H_2S Tedlar bag, (2) CO_2-containing cylinder, (3) air compressor, (4) peristaltic pumps, (5) valves, (6) rotameters, (7) mixing unit, (8) mixing chamber, (9) biotrickling filter, (10) pH controller, (11) NaOH solution (2 M), (12) 1 L nutrient-feeding reservoir, (13) magnetic stirrer. Legend: BTF_H – biotrickling filter with "high" media surface area, BTF_L – biotrickling filter with "low" media surface area.

and 500 mL (Stage III) of solution every 24 h. A portable magnetic stirrer was used to mix the MSM solution. Both systems were operated with daily renewal of a nitrate-rich trickling solution.

2.3. Analytical methods

2.3.1. Gas phase monitoring

Gas samples containing CO_2, N_2, H_2S, and O_2 were collected daily from the inlet (downstream of the mixing chamber unit) and outlet of the BTF systems in duplicate and, measured in a gas chromatograph (Model 8890 Agilent Technologies, Santa Clara, CA, USA). The thermal conductivity detector and injector temperatures were maintained constant at 170°C and 160°C, respectively, for 5 min. Helium was used as the carrier gas at 13.7 mL min^{-1}.

2.3.2. Liquid phase monitoring

The concentration of total organic carbon (TOC), inorganic carbon (IC), total nitrogen (TN), nitrite (NO_2), nitrate (NO_3), sulfate (SO_4), and thiosulfate (S_2O_3) ions were analyzed three times a week in the recirculating aqueous solution. TOC, IC and TN analyses were performed in a TOC-VCSH analyzer coupled with a TNM-1 chemiluminescence module (Shimadzu, Japan). The pH was automatically monitored and controlled at a setpoint of 7.0 using a pH dosing device (model EVO pH-P, BS Pool, Barcelona, Spain) connected to a 200 mL flask containing 2 M NaOH. Nitrite, nitrate, sulfate, and thiosulfate concentrations were determined by HPLC-IC using a Waters 515 HPLC pump, a conductivity detector (Waters 432), an IC-PAK Anion HC column (4.6 × 150 mm), and an IC-Pak Anion Guard-Pak (Waters). The samples were filtered through 0.22 µm pore-size membranes before anion analysis. The sulfide content was measured using a highly sensitive photometric method (Merck KGaA, Darmstadt, Germany) for the quantification of HS^- and S^{2-} ions in the range of 0.02 – 1.55 mg L^{-1}. Volatile suspended solids (VSS) were analyzed according to the Standard Methods for the Examination of Water and Wastewater [5].

2.4. Abiotic test

Prior to inoculation of the BTFs, a 9-day abiotic test was carried out without filler material, in which the gas concentrations at the inlet and outlet of the BTFs were monitored. The packing material was then introduced into the systems and the potential H_2S abiotic removal via adsorption was assessed over a period of four consecutive days.

2.5. Statistical analysis

A statistical analysis was performed to compare the performance of both BTF_H and BTF_L across three operating stages. The parameters compared included elimination capacities (EC), sulfate production, and the nitrate-oxygen contribution to H_2S oxidation. Due to the non-normal distribution of the data, a non-parametric Mann-Whitney U Test was employed to assess differences between the two systems at each stage. Statistical significance was set at $p < 0.05$. All analyses were conducted using Statistica software.

2.6. Calculations

The H_2S loading rates (LR) (g-H_2S m^{-3} h^{-1}) during operation were calculated using Eq. (1), where Q_{gas} is the biogas flow rate (m^3 d^{-1}), $Q_{air,in}$ is the inlet air flow rate (m^3 d^{-1}) applied to the systems, C_{in} is the inlet concentration of H_2S (g m^{-3}), and V is the packed bed reactor volume (m^3). The H_2S-EC (g-H_2S m^{-3} h^{-1}) of the BTFs during the entire operation were calculated using Eq. (2), where Q_{gas} represents the biogas flow rate (m^3 d^{-1}), $Q_{air,in}$ is the inlet air flow rate (m^3 d^{-1}) applied to the systems, C_{in} is the inlet concentration of H_2S (g m^{-3}), and V is the packed bed reactor volume (m^3). The H_2S removal efficiencies (RE, %) were calculated according to Eq. (3), where Q_{in} and Q_{out} are the biogas-air mixtures flow rates (L d^{-1}) at the inlet and outlet of the BTFs, respectively, and C_{in} and C_{out} are the concentrations (%) of H_2S in the biogas at the inlet and outlet of the BTFs, respectively. If complete H_2S removal is achieved, consider LR = EC.

$$LR = \frac{(Q_{gas} + Q_{air,in}) \times C_{in}}{V} \quad (1)$$

$$EC = \frac{(Q_{gas} + Q_{air,in}) \times (C_{in} - C_{out})}{V} \quad (2)$$

$$RE = \frac{(C_{in} - C_{out})}{C_{in}} \times 100 \quad (3)$$

Since H_2S was continuously introduced into the gas phase, while nitrate was refreshed in a semi-continuous mode within the liquid phase, all calculations were standardized by accounting for both components on a common basis: moles per day. This approach ensured consistency in assessing the system's performance and avoided inaccuracies associated with direct volume-based comparisons due to phase-dependent properties. The moles of H_2S removed per day were determined from the gas flow rate and concentration measurements using the ideal gas law, while nitrate consumption was calculated from the volumetric replacement and concentration difference of the trickling solution.

The consumption of nitrate (mol d^{-1}) throughout the operating period was calculated according to Eq. (4), where V_{liquid} is the total volume of the trickling solution inside the BTF (m^3), $C_{in,\ NO3}$ and $C_{out,\ NO3}$ (mol m^{-3}) are the initial and final concentrations of nitrate per cycle (24 h). Assuming that the liquid trickling solution is well-mixed, and nitrate is evenly available throughout the reactor with no side reactions, the biological H_2S oxidation by nitrate (mol d^{-1}) was calculated using Eq. (5), where N/S is the nitrogen/sulfur ratio based on the stoichiometry from the anaerobic oxidation reactions. The total H_2S (mol d^{-1}) removed from the BTFs was calculated using Eq. (6), where Q_{gas} is the volumetric inlet biogas-air flow rate (m^3 h^{-1}), $C_{in,\ H2S}$ and $C_{out,\ H2S}$ (mol m^{-3}) are the inlet and outlet concentrations of H_2S, and t is the time per each cycle (24 h). Assuming that the gas mixture is mostly inert N_2 and CO_2 with low levels of H_2S, the number of moles of H_2S (mol) in 1 m^3 (mol m^{-3}) at the inlet and outlet of the BTFs was calculated following Eq. (7) and Eq. (8), where P_{H2S} is the partial pressure of H_2S (atm), Q_{gas} is the volumetric biogas-air flow rate (m^3 h^{-1}), Δt is duration of each cycle (h), R is the universal gas constant (8.314 J mol^{-1} K^{-1} or 0.0821 L atm mol^{-1} K^{-1}), T is the operating temperature (K), and P_{total} (atm) is the total pressure in the BTFs.

$$NO_3 consumed\ (mol/day) = V_{liquid} \times (C_{in,NO3} - C_{out,NO3}) \times t \quad (4)$$

$$\text{Total } H_2S \text{ oxidized by nitrate } (mol/day) = \frac{NO_3 consumed\ (mol/day)}{N/S \text{ from stoichometry}} \quad (5)$$

$$\text{Total } H_2S \text{ removed } (mol/day) = Q_{gas} \times (C_{in,H2S} - C_{out,H2S}) \times t \quad (6)$$

$$P_{H_2S} = \frac{H_2S \text{ mole fraction}}{10^6} \times P_{total} \quad (7)$$

$$\text{Moles of } H_2S_{(inlet/outlet)} = \frac{P_{H_2S,inlet/outlet} \times Q_{gas} \times \Delta T}{R \times T} \quad (8)$$

The proposed mass balance for the BTFs evaluated the conversion of gaseous H_2S in various sulfur compounds in the aqueous phase, as described in Eq. (9). More specifically, the total cumulative H_2S removed from the gas phase, $H_2S(g)$, was determined by the sum of the sulfur species accumulated in the liquid phase, including total dissolved sulfide (TDS), sulfate (SO_4), thiosulfate (S_2O_3), and elemental sulfur (S^0), subtracting the sulfate fraction ($MgSO_4$) supplied in the MSM. To accurately assess the long-term accumulation of S^0 and ensure precise

mass balance calculations, elemental sulfur was not washed out from the reactors. Instead, it was allowed to accumulate within the system to provide a reliable measure of sulfur deposition over time, which is critical for understanding the performance and stability of the biotrickling filters under high H_2S loads. The nitrate contribution (%) to the total oxidation of H_2S was measured using Eq. (10).

$$H_2S_{(g,inlet-outlet)} = \left[\sum (TDS + SO_4 + S_2O_3 + S^0) - MgSO_{4\,added}\right]_{(aq,accumulated)} \quad (9)$$

$$NO_3 contribution\ (\%) = \frac{H_2S\ oxidized\ by\ nitrate}{Total\ H_2S\ removed} \quad (10)$$

3. Results and discussion

3.1. Effect of the EBRT on H_2S removal

The effect of the EBRT on H_2S removal efficiency was investigated at constant inlet H_2S concentrations and O_2:H_2S ratios in both BTF_H (9.5 ± 0.6 gS-H_2S m^3 and 24.4 ± 1.8, respectively) and BTF_L (9.3 ± 0.6 gS-H_2S m^3 and 24.4 ± 1.5, respectively). Complete H_2S removal was achieved by the BTFs within 48 h after inoculation, with efficiency maintained even under the shortest EBRT (Stage III, 4 min) (Fig. 2 a – b), demonstrating the robustness and efficiency of the immobilized microbial community in handling high inlet sulfur loads. A 15 % reduction (from 137 ± 3–117 ± 3 gS-H_2S m^{-3} h^{-1}) in the H_2S-EC of BTF_H was observed under the shortest EBRT and at the highest inlet biogas flow rate (360 L d^{-1}), however, no statistical differences with the BTF_L were observed at any operating stages (Fig. 2 **c – d**). According to Pudi et al. [73], the operation of a BTF at low EBRT typically results in an increased inlet LR, which can enhance BTF elimination capacity. However, very high H_2S mass flowrate may saturate the capacity of the biofilm to oxidize the pollutant, thus limiting the BTF's capacity to degrade the increased load, ultimately leading to a reduction in H_2S-RE under long-term operation.

In our case, the BTF_H packed with Kaldnes K1 Micro rings exhibited a trade-off between surface area benefits and operational stability. Although the higher specific surface area of the micro rings entailed an adequate void space for microbial attachment and biofilm growth,

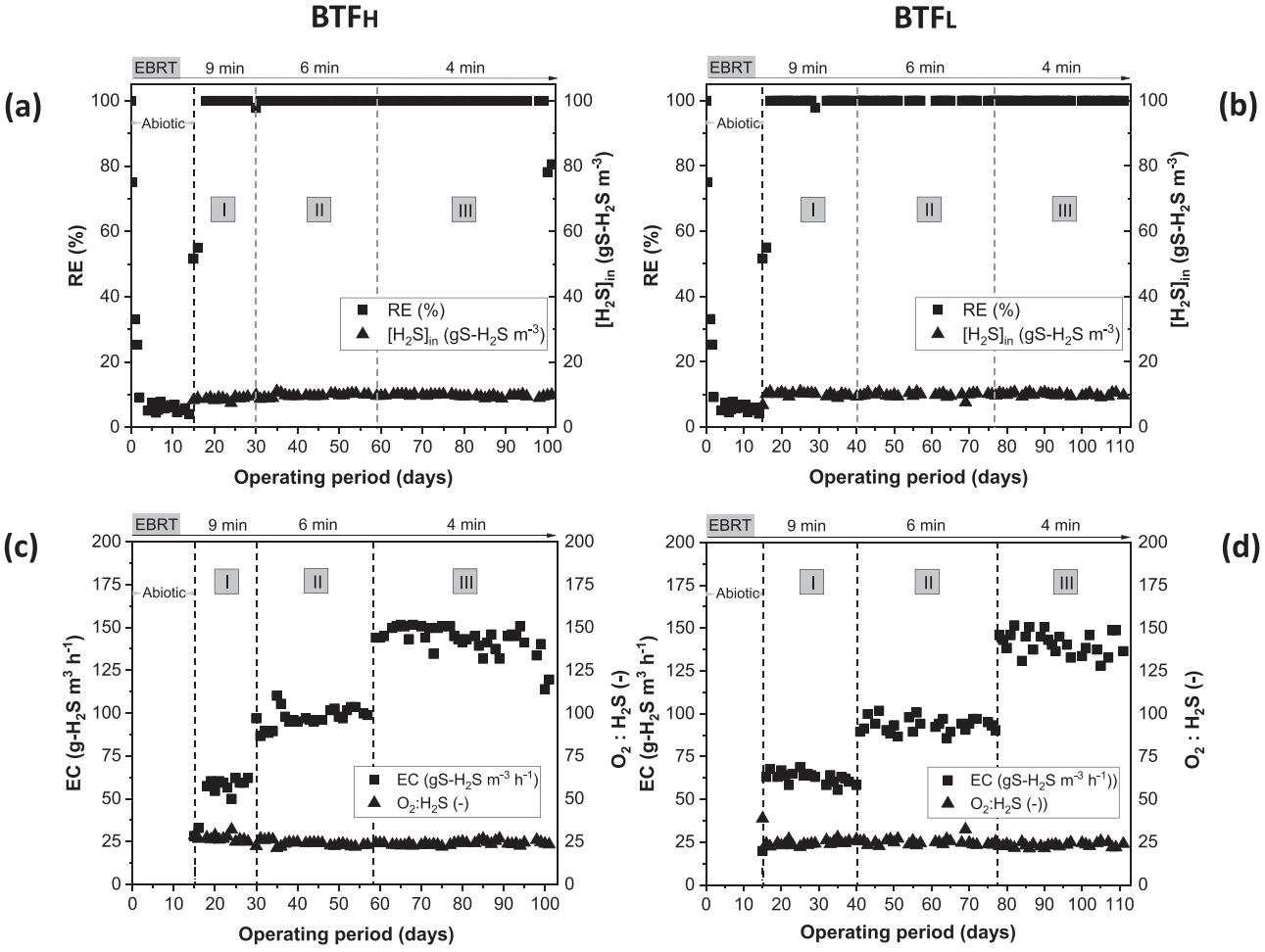

Fig. 2. Time course of H_2S biological oxidation in the BTFs in terms of: (a – b) H_2S removal efficiencies (RE, %) and (c – d) H_2S elimination capacities (ECs, g-H_2S m^{-3} h^{-1}).

potentially boosting H_2S oxidation rates, the reduced bulk porosity fostered the accumulation of S^0 and biomass under moderate EBRT conditions. Indeed, when the EBRT was reduced and the H_2S loading rate increased, this thickened biofilm became prone to clogging, which ultimately limited the BTF performance and stability. Consequently, the BTF_H did not outperform BTF_L under high H_2S loads, which highlights the importance of selecting packing materials that balance biofilm development with long-term operational stability. In more demanding operational scenarios, such as the high H_2S flow rates from acidogenic systems (e.g. sugarcane vinasse dark fermentation), the balance between surface area for enhanced mass transfer without clogging and the ability to support biofilm growth becomes crucial.

The impact of decreasing the EBRT on reactor performance has been extensively studied in aerobic BTFs for H_2S removal under moderate to high loading rates in neutral or alkaline conditions. In Fig. 3, the relationship between H_2S-RE and inlet H_2S-LR is illustrated, with the size of the circles indicating the EBRT for each study. A summary of studies on SOB treating H_2S in aerobic BTFs packed with distinct support media is also provided in Table S1 (Supplementary Material). In BTF systems inoculated with activated sludge from WWTPs and packed with metallic Pall rings, Montebello et al. [63,62] reported maximum H_2S elimination capacities (ECs) of 52.0 and 51.5 gS-H_2S m^{-3} h^{-1}, achieving H_2S removal efficiencies of 99 % and 100 % at EBRTs of 180 s and 131 s, respectively. In a prior study, Montebello et al. [61] reported a lower H_2S-RE of 68 % using HD-QPAC® at a higher LR of 215 gS-H_2S m^{-3} h^{-1} and EC (160 gS-H_2S m^{-3} h^{-1}) in a BTF operated at an EBRT of 180 s. Similarly, Qiu and Deshusses [74] observed an EC of 122 gS-H_2S m^{-3} h^{-1} at an EBRT of 41 s in a BTF packed with honeycomb monolith, corresponding to a LR of 127 gS-H_2S m^3 h^{-1} and a RE of 95 %. Similarly, maximum ECs of 237 and 386 gS-H_2S m^{-3} h^{-1} were reported by López et al. [56] and Wu et al. [94] at EBRTs of 118 and 60 s, respectively, associated with H_2S-REs higher than 80 %. According to Wu et al. [94], the slightly alkaline conditions of the recirculating medium might have enhanced the mass transfer of H_2S from the gas to the liquid phase, thus preventing the toxic effects of 5000 ppm_v H_2S on SOB populations. In the present study, the treatment of ~ 7000 ppm_v H_2S (~10.0 gS-H_2S m^{-3}) with sustained, long-term 100 % H_2S-RE at a low EBRT of 4 min confirmed the significant potential of biotrickling filters for the treatment of gas emissions from acidogenic reactors treating high SO_4 strength wastewaters such as sugarcane vinasses.

In the hybrid aerobic-anoxic trickling systems, both CO_2 and O_2 concentrations were closely monitored to assess their variations throughout the operation. For the BTF_H, the inlet CO_2 content was 11.9 ± 0.9 %, while the outlet CO_2 concentration increased slightly to 12.1 ± 1.1 %. In contrast, O_2 concentrations decreased from 17.7 ± 0.2 % at the inlet to 17.0 ± 0.4 % at the outlet, likely due to the transfer of O_2 to the liquid phase. Correspondingly, N_2 levels increased from 69.7 ± 0.8 % at the inlet to 70.9 ± 0.8 % at the outlet, which could be attributed to simultaneous autotrophic denitrification. Similarly, in BTF_L, CO_2 concentrations showed a modest increase from 12.7 ± 1.7 % at the inlet to 13.1 ± 1.7 % at the outlet, while O_2 concentrations decreased from 17.2 ± 0.2 % to 16.5 ± 0.4 %. N_2 levels in BTF_L also increased, from 69.3 ± 1.2 % at the inlet to 70.5 ± 1.4 % at the outlet. The dynamics of acidogenic off-gas composition throughout the operational period are depicted in Fig. 4 **a – d**, illustrating the temporal variations in CO_2, O_2, H_2S and N_2 concentrations in both BTF configurations.

Fermentative reactors processing sugarcane vinasse often generate significant amounts of H_2S due to their highly active sulfidogenic microbial community [12,33], which requires additional treatment of the acidogenic biogas to prevent corrosion and occupational hazards. Our study demonstrated that complete oxidation of H_2S in BTFs can be effectively achieved, providing a viable solution for treating high-strength H_2S streams. This method allows for an efficient treatment of H_2S at relatively short gas contact times, thereby reducing the need for larger reactor volumes (which is valuable for industrial applications with space constraints) and minimizing associated construction costs. This approach could also help mitigating environmental issues associated with high H_2S emissions, thereby reducing the environmental footprint and improving air quality. In a real scenario, CO_2 is naturally generated from sugarcane vinasse processing, eliminating the need for costly external inorganic carbon supplements, such as bicarbonate, which are typically required to support the growth of autotrophic populations in BTFs [94,31,63,61,62]. Moreover, while introducing air to conventional BTFs for biomethane upgrading can dilute the methane content and create explosive atmospheres in biogas from methanogenic systems, this dilution is not a concern for sulfide-rich acidogenic off-gas from sugarcane fermentation. Since acidogenic reactors in 2nd-AD systems prioritize fermentation over methane production, supplying air to the acidogenic biogas for H_2S oxidation aligns well with the operational goals.

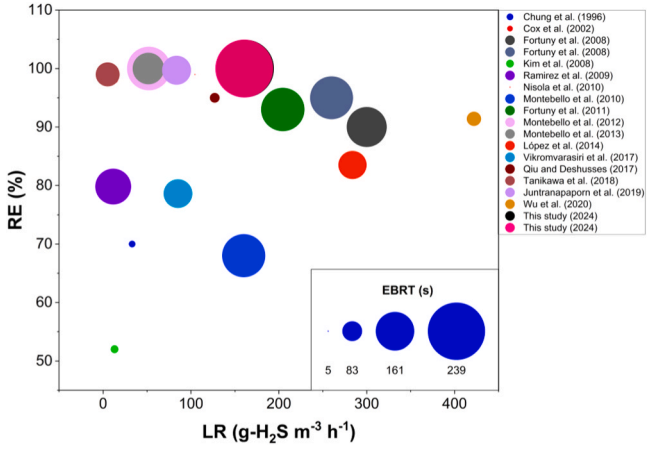

Fig. 3. Comparison of H_2S removal efficiency (RE) versus the influent loading rate (LR) for literature studies, including the current study. **Notes**: The size of the circles represents the empty bed residence time (EBRT) of the aerobic biotrickling filters used in each study, with larger circles indicating longer EBRT. Data points represent findings from previous research, with color coding to differentiate among studies [19,21,43,47,89,91].

3.2. *MSM supply strategies for enhanced simultaneous denitrification and H_2S oxidation*

In the BTF_H, TOC concentrations remained consistently below 50 mg L^{-1} throughout the operating stages. This low TOC level is attributed to the initial addition of microalgae and activated sludge during inoculation, as no additional carbon source was introduced during the continuous operation. The IC concentrations in BTF_H reached an average of 129 ± 31 mg L^{-1}, primarily due to the mass transfer of CO_2 from the gas stream into the liquid phase. In BTF_L, TOC and IC concentrations were slightly higher, with TOC averaging 77 ± 53 mg L^{-1} and IC reaching 160 ± 31 mg L^{-1}. These differences between BTF_H and BTF_L can be attributed to variations in gas-liquid interactions and microbial activity within each system.

At the beginning of the operation, nitrate depletion was observed in BTF_H (from 115 to 9 mgN-NO_3 L^{-1}) and BTF_L (from 96 to 4 mgN-NO_3 L^{-1}), with a complete nitrate consumption occurring after 5 and 9 days, respectively (Fig. 5 **a – b**). NO_2 concentrations remained below the quantification limits in both systems, indicating minimal accumulation of this intermediate. Based on these findings, a MSM feeding strategy was implemented, which involved the replacement of MSM to maintain a simultaneous H_2S oxidation and autotrophic denitrification in both systems and help offsetting O_2 mass transfer limitations. Thus, average daily nitrate concentrations in the BTF_H and BTF_L of 9 ± 1 mgN-NO_3 L^{-1} (Stage I), 28 ± 2 mgN-NO_3 L^{-1} (Stage II) and 42 ± 5 mgN-NO_3 L^{-1} (Stage III) were restored throughout the operating period in both BTFs.

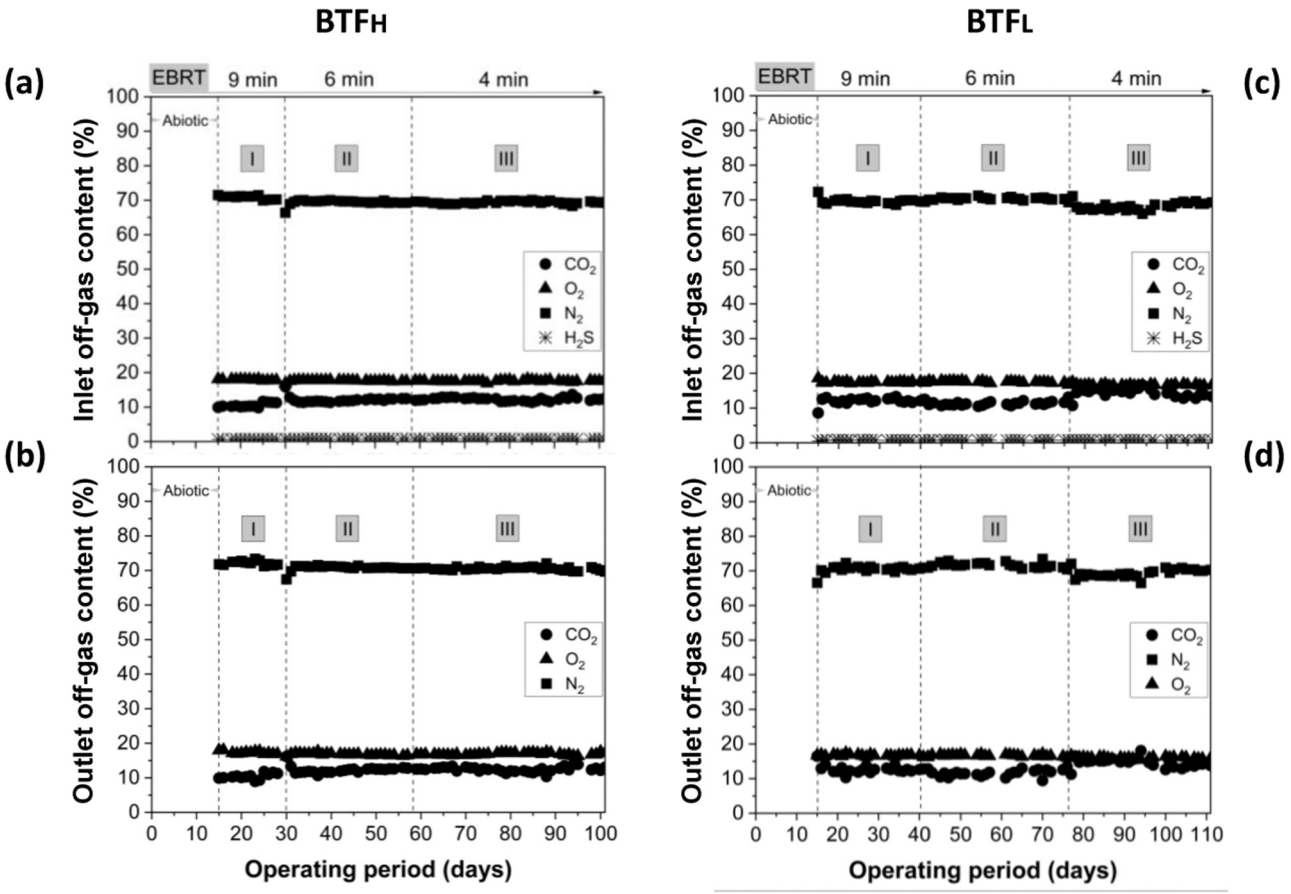

Fig. 4. Time course of the acidogenic-off gas content (%) at the inlet and outlet zones of the BTFs.

The comparative analysis of nitrate consumption between the two systems revealed no statistically significant differences in input nitrate levels ($p < 0.05$) across the operating stages.

In BTF_H, the high specific area of the K1 Kaldnes rings offered a large surface for microbial attachment, allowing nitrate-reducing sulfur-oxidizing bacteria (NR-SOB) to thrive despite fluctuations in H_2S loads, keeping H_2S-RE of 100 %, despite limited long-term stability. This finding supports the adaptability of the system to changing conditions, which is crucial for their industrial deployment. In Stages I and II, pH levels were maintained close to neutrality with NaOH supply rates of 2.8 ± 0.6 and 4.0 ± 0.2 g-NaOH d^{-1}, respectively. However, packing media clogging at the highest H_2S flow rate (Stage III) was observed due to excessive deposition of S^0 across the packed bed and at the base of the biofilter. As a result, a malfunction in the pH controller resulted in an unregulated pH drop to ~ 2.0 (Fig. 5 **c**) from the accumulation of proton ions generated by the complete oxidation of H_2S to sulfate [17]. This sharp decrease in pH likely inhibited NR-SOB activity, causing nitrate reduction to halt temporarily and leading to an accumulation of nitrate in the solution. The lack of nitrate consumption, reflected in Fig. 5 **a** as a plateau or increase in nitrate levels, corresponds to this period of pH disruption. NaOH was then manually added to raise the pH to neutral levels to stabilize the system. Introducing a fresh inoculum at 10 % of the initial volume further supported system stability by enhancing nitrate reduction and sulfide oxidation. Both interventions allowed nitrate reduction to resume and NaOH consumption rates to stabilize at 5.8 ± 0.2 g-NaOH d^{-1} under the maximum H_2S load herein tested, as NR-SOB activity was restored, and nitrate levels began to decrease again. Even though the system mainly operated under aerobic conditions, nitrate helped supporting a consistent sulfide oxidation, especially given the underlying O_2 transfer limitations occurring the BTFs because of the low solubility of O_2 in water compared to H_2S [15,4]. The rapid nitrate consumption patterns supported the hypothesis of oxygen limitation, when nitrate served as the primary electron acceptor rather than exclusively as a nitrogen source.

In contrast, BTF_L maintained a relatively stable pH throughout the operation without external intervention. This stability suggests that the higher bulk porosity of the polyhedral balls led to lower rates of H_2S oxidation, thus preventing the packed bed from clogging. The consistent nitrate reduction in BTF_L, as shown in Fig. 5 **b**, indicates a steady NR-SOB activity. NR-SOB are commonly found in different water environments with abundant reduced sulfur compounds and limited oxygen, including WWTPs [51]. These microorganisms rely on inorganic carbon as a carbon source (i.e., CO_2, HCO_3^-) and oxidize sulfur compounds (i.e., H_2S, S_2O_3, S^0) for energy production via the autotrophic denitrification pathway [49]. Enzymatic activity in both sulfide oxidation and nitrate reduction can be pH-dependent, with neutral to slightly alkaline conditions typically favoring the enzymes responsible for these metabolic pathways. Deng et al., [24]. Besides, maintaining neutral or slightly alkaline conditions in biotrickling filters prevents pH-related bio--toxicity incidents [94], enhances H_2S solubility [14] and cell activity [46], and reduces corrosion risks, the latter increasing maintenance costs and reducing the lifespan of BTFs [99]. In contrast, acidic pH levels may result in reduced growth rates, impaired enzyme function, or even cell damage, leading to decreased H_2S oxidation to sulfate (SO_4) and nitrate reduction to nitrogenous gases (e.g. N_2 or N_2O) [14].

Most studies on aerobic desulfurization systems without nitrate have been conducted at lower H_2S loading rates (5.2 – 104.5 gS-H_2S m^{-3} h^{-1}) (Table S1 – Supplementary Materials), which differ significantly from the higher loading rates (>160 gS-H_2S m^{-3} h^{-1}) managed in the anoxic-aerobic system described here. At these high rates, the combined effect of nitrate supplementation and lower surface area packing media was essential for maintaining system efficiency and preventing sulfur build-

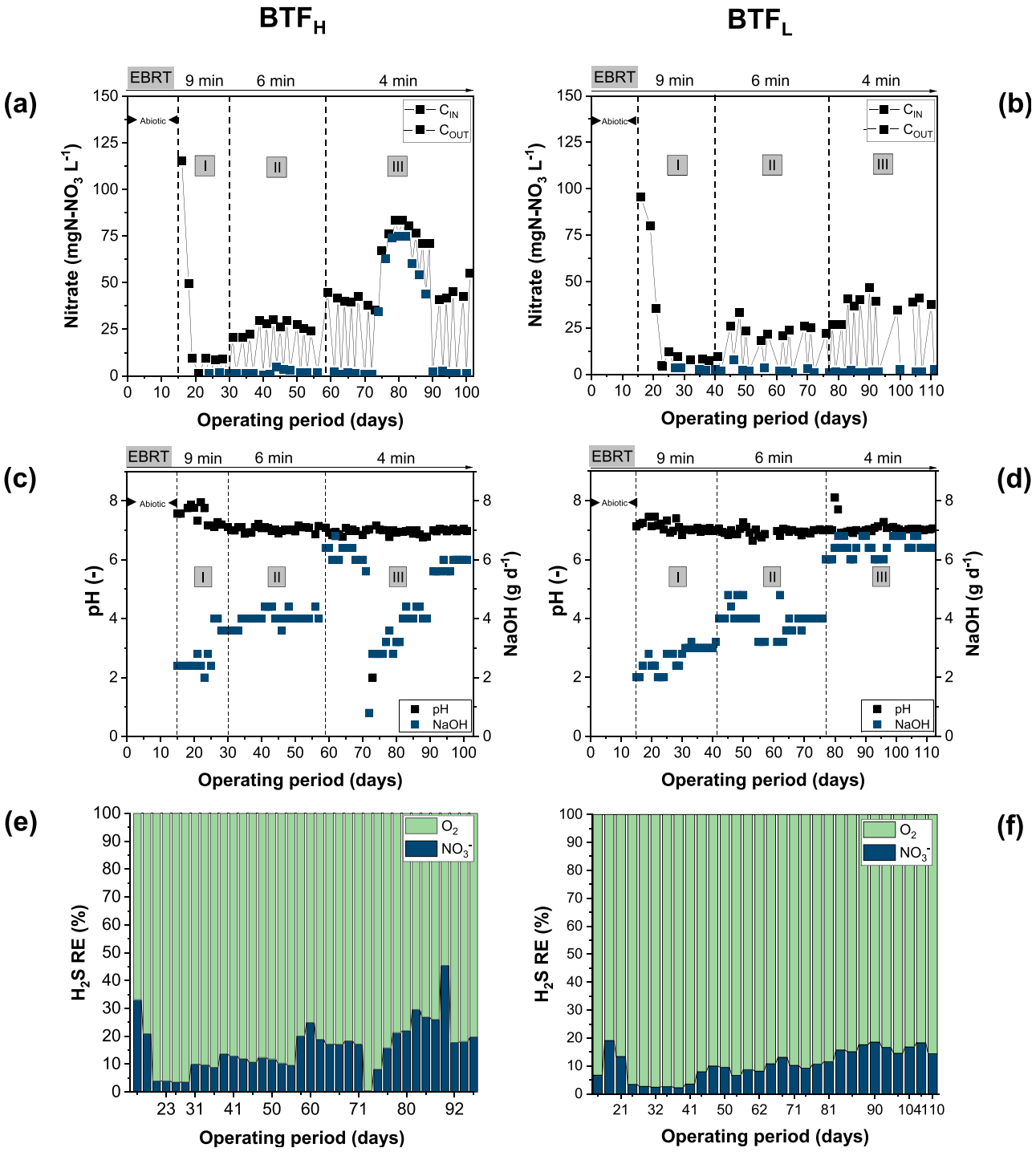

Fig. 5. Time course of: (a – b) nitrate concentrations, (c – d) pH and NaOH consumption, and (e – f) electron acceptors (O_2 and NO_3) contribution to the total oxidation of sulfide.

up. In contrast, studies such as those by Fortuny et al. [31,32] at higher loading rates (259 – 300 gS-H_2S m^{-3} h^{-1}) without nitrate supplementation reported severe operational challenges, such as high pressure drops and clogging. Therefore, the integration of nitrate, alongside optimized packing media, offers a dual strategy that enhances resilience and ensures consistent performance under high H_2S-load conditions.

Several studies have reported lower H_2S-LR and H_2S-EC compared to this study, highlighting different performance levels in anoxic desulfurization systems (Table S2 – Supplementary Materials). Zeng et al. [97] observed a maximum EC of 30.7 gS-H_2S m^{-3} h^{-1} associated with a RE of 84.7 % in a BTF packed with pall rings and inoculated with *Thiobacillus* and *Sulfurimonas* species. In BTFs inoculated with activated sludge, Bayrakdar et al. [9] achieved a maximum EC of 45 gS-H_2S m^{-3} h^{-1} with a RE of 98 % using activated carbon as the packing material. Li et al. [53] reported a maximum EC of 54.5 gS-H_2S m^{-3} h^{-1}, achieving 100 % RE using polypropylene packing material. Soreanu et al. [86] demonstrated an EC up to 14.5 gS-H_2S m^{-3} h^{-1}, with complete H_2S removal using plastic fiber. More recently, Severi et al. [85] reported a maximum EC of 47.4 gS-H_2S m^{-3} h^{-1} and a H_2S-RE of 84.4 % under an inlet H_2S concentration of 11,023 ppm_v and an EBRT of 21.4 min.

When comparing studies with similar or higher H_2S-LR, the performance of this study remains competitive. Almenglo et al. [3] reported a

maximum EC of 140 gS-H_2S m^{-3} h^{-1} with a RE of 84 % in a BTF inoculated with *Sedimenticola*. Zeng et al. [96] achieved an EC of 81.3 gS-H_2S m^{-3} h^{-1} and a RE of 94.5 % using PU foam and hollow balls as packing materials. Both Fernandez et al. [30] and Fernandez et al. [29] reported ECs of around 170–171 gS-H_2S m^{-3} h^{-1} with REs of 85 % in BTFs packed with activated sludge and PU foam, respectively. Cano et al. [15] attained a high EC of 287 gS-H_2S m^{-3} h^{-1} and a RE of 99 % in a BTF inoculated with anaerobic sludge. Although the need for an electron acceptor (i.e. nitrate) can increase the operating costs of biodesulfurization units, the implementation of additional NO_3 supply to stimulate autotrophic denitrification is often reported in the literature as a result of the multiple benefits: (i) reduced biomass production rates, which decreases biomass disposal requirements, prevents clogging in BTF and increases the lifespan of the packing material [28]; (ii) higher tolerance to high H_2S loads [4]; (iii) compatibility with existing nitrogen-rich wastewater [16,39,38,84]; (iv) effective control of pH [78], and (v) improved sulfate selectivity due to minimized oxygen transfer limitations at high H_2S loads [29]. Hence, the engineering of aerobic-anoxic BTFs systems is aligned with the development of low environmental footprint sugarcane biorefineries since the nitrate required might be produced from the oxidation of the NH_4^+ present in the wastewaters of the biorefineries, which would mitigate their potential eutrophication impacts.

Nitrate-driven systems facilitate the partial or complete oxidation of H_2S to sulfate, which can be managed more easily in liquid form than S^0, which tends to clog the filter media [4]. According to Lenis et al. [52], the complete anaerobic oxidation of H_2S to sulfate coupled with nitrate reduction to N_2 gas remain stable at N/S molar ratios $\geq$ 1.6. When nitrate concentrations are low, external dosing can be applied, but it must be carefully controlled to minimize operational costs [13,44]. In this context, Fernández et al. [29] reported N:S ratios ranging from 0.47 to 1.61 mol-N mol^{-1}-S with sulfate selectivity ranging from 3 % to 82 %. Similarly, Almengló et al. [3] reported a decreasing S^0 production under anoxic conditions from 92 % to 5 % by increasing the available nitrate from 0.34 to 1.74 mol-N mol^{-1}-S. At similar LR (173.2 gS-H_2S m^{-3} h^{-1}) and inlet H_2S concentrations (6000 ppm_v) used in this study, the authors concluded that N/S molar ratios below 0.4 mediated a negligible effect on H_2S-RE, although an increase in S^0 production was anticipated. Accordingly, the N/S molar ratios set in both BTFs in this study remained at 0.1, 0.3, and 0.5 during Stages I, II, and III, respectively, likely favoring S^0 accumulation, as indicated in Eq. (10), without compromising the efficiency of the systems. However, the continuous supply of O_2 in the gas phase mitigated this phenomenon.

$$5HS^- + 2NO_3^- + 7H^+ \rightarrow 5S^0 + N_2 + 6H_2O \ (\Delta G^0 = -1264 kJmol^{-1}) \quad (10)$$

The greatest contribution of nitrate to H_2S oxidation (33 and 19 %) occurred at the start of the operation in BTF_H and BTF_L, respectively, before the trickling solution was renewed. At this stage, nitrate concentrations from the inoculum sources (i.e. algal-bacterial biomass and activated sludge) and MSM were initially high, thus supporting a high nitrate availability to the microbial consortia. Fig. 5 **e – f** depicts the contribution (%) of the electron acceptors (O_2 and NO_3) to the total oxidation of H_2S for both BTFs. Thus, nitrate contribution to sulfur oxidation in BTF_H increased across the three operational stages, with values of 3.8 ± 0.2 %, 11.1 ± 1.5 %, and 19.1 ± 2.6 % in Stages I, II, and III, respectively. Conversely, the corresponding contributions in BTF_L were slightly lower, reaching 2.7 ± 0.4 %, 9.4 ± 1.7 %, and 15.4 ± 2.4 %. Notably, no statistical differences were observed in the nitrate contribution to H_2S oxidation between the systems during Stages I and II. However, at higher H_2S loads (Stage III), BTF_H exhibited a greater nitrate contribution, likely due to localized oxygen limitations, leading to an increased reliance on nitrate. Interestingly, the greatest nitrate contribution in BTF_H may also have facilitated elemental sulfur accumulation at the highest H_2S flow rates under a N/S ratio of 0.5, leading to clogging.

3.3. Oxidized species accumulation

BTF_H exhibited higher TDS concentrations in the liquid phase, reaching up to 3.6 mgS^{2-} L^{-1}, compared to a maximum of 0.4 mgS^{2-} L^{-1} in BTF_L. TDS concentrations remained low and stable throughout the experimental period, which emphasizes the efficient uptake of sulfide by the consortia even at increasing H_2S loading rates. Thiosulfate (S_2O_3) ions were detected shortly after the initial start-up of the BTF_H, peaking at 1.5 gS-S_2O_3 L^{-1} on day 18th, with no subsequent accumulation from this day onwards (Fig. 6 **a – b**). In Stage I, sulfate (S-SO_4) concentrations in the trickling solution gradually increased, reaching up to 8.6 gS-SO_4 L^{-1} in BTF_H and 10.6 gS-SO_4 L^{-1} in BTF_L, accounting for 53 and 38 % of the total inlet H_2S concentrations applied to the BTFs, respectively, exhibiting no statistical differences between the systems. These findings suggest that the biological oxidation of H_2S predominated over its physical absorption into the trickling liquid, leading to the rapid accumulation of sulfate and S^0 in the systems. Temporal profiles of cumulative sulfur oxidized species (mainly sulfate) relative to the total cumulative inlet gaseous H_2S are presented in Fig. 6 **a – b**.

The reduction of the gas-liquid contact time at decreasing EBRTs in both BTFs drastically resulted in a lower sulfate accumulation associated with enhanced S^0 generation possibly due to O_2 mass transfer limitations in the filter bed. During Stage II, only 5 and 6 % of the total inlet H_2S concentrations were converted into sulfate in BTF_H and BTF_L, respectively. At the highest H_2S loading (> 140 gS-H_2S m^{-3} h^{-1}), the average sulfate concentrations in BTF_H and BTF_L reached 4.5 ± 1.1 gS-H_2S m^{-3} and 3.9 ± 0.8 gS-H_2S m^{-3} at conversion of H_2S to S^0 > 98 %, corresponding to the accumulation of 192 gS-S^0 and 154 gS-S^0 in the packed bed, respectively. Again, no statistical differences were observed between the systems during Stages II and III. The higher denitrification activity in BTF_H (Fig. 5 **e)** may have contributed to a higher cumulative sulfur precipitation. In this context, a decrease in the ratio of S-SO_4 due to the decreased EBRT at fixed H_2S concentrations and O_2:H_2S ratios are also typically reported in the literature [31,76,94]. Indeed, López et al. [56] reported a reduced sulfate selectivity associated with a stepwise LR increase up to 283.8 gS-H_2S m^{-3} h^{-1} in a BTF system packed with plastic pall rings at neutral pH and inoculated with aerobic sludge from a municipal WWTP, even at a higher O_2:H_2S ratio of 41.2 (v v^{-1}) compared to the present study. According to the authors, regulating the trickling liquid velocity improved dissolved oxygen distribution along the packed bed height, thus enhancing the overall desulfurization performance. Jaber et al. [40] observed a reduction in sulfate selectivity from 90 % to 59 % associated with an increase in the inlet H_2S concentration from 150 to 600 ppm_v at a constant N/S molar ratio of 0.89 mol mol^{-1}. In fact, when high H_2S loads are treated, difficulties in achieving high dissolved oxygen levels in the liquid phase are commonly reported in the literature, leading to the formation of cream-whitish layers of elemental sulfur in the packed bed [31,64,78]. Similarly, Zhang et al. [98] reported clogging issues by excess S^0 generation in a biological desulfurization unit when the inlet H_2S concentrations were above 700 ppm_v, which were ten times lower than the H_2S concentrations used in this study.

The primary objective of this study was to maximize sulfate production as the target oxidation species, although elemental sulfur formation was an anticipated outcome due to the high H_2S concentrations (7000 ppm_v) to be treated. While Fortuny et al. [31] reported a lower sulfate production under similar conditions, subsequent optimization by Fortuny et al. [32] achieved higher sulfate yields with a modified O_2:H_2S ratio to 23.6 v v^{-1}. Despite adopting a similar ratio of 24.0 in our systems, elemental sulfur accumulation was unavoidable, resulting in a complete H_2S removal. The BTFs were operated sequentially, and when BTF_H experienced clogging due to increased sulfur accumulation, the packing media was changed to assess its impact on sulfur build-up and

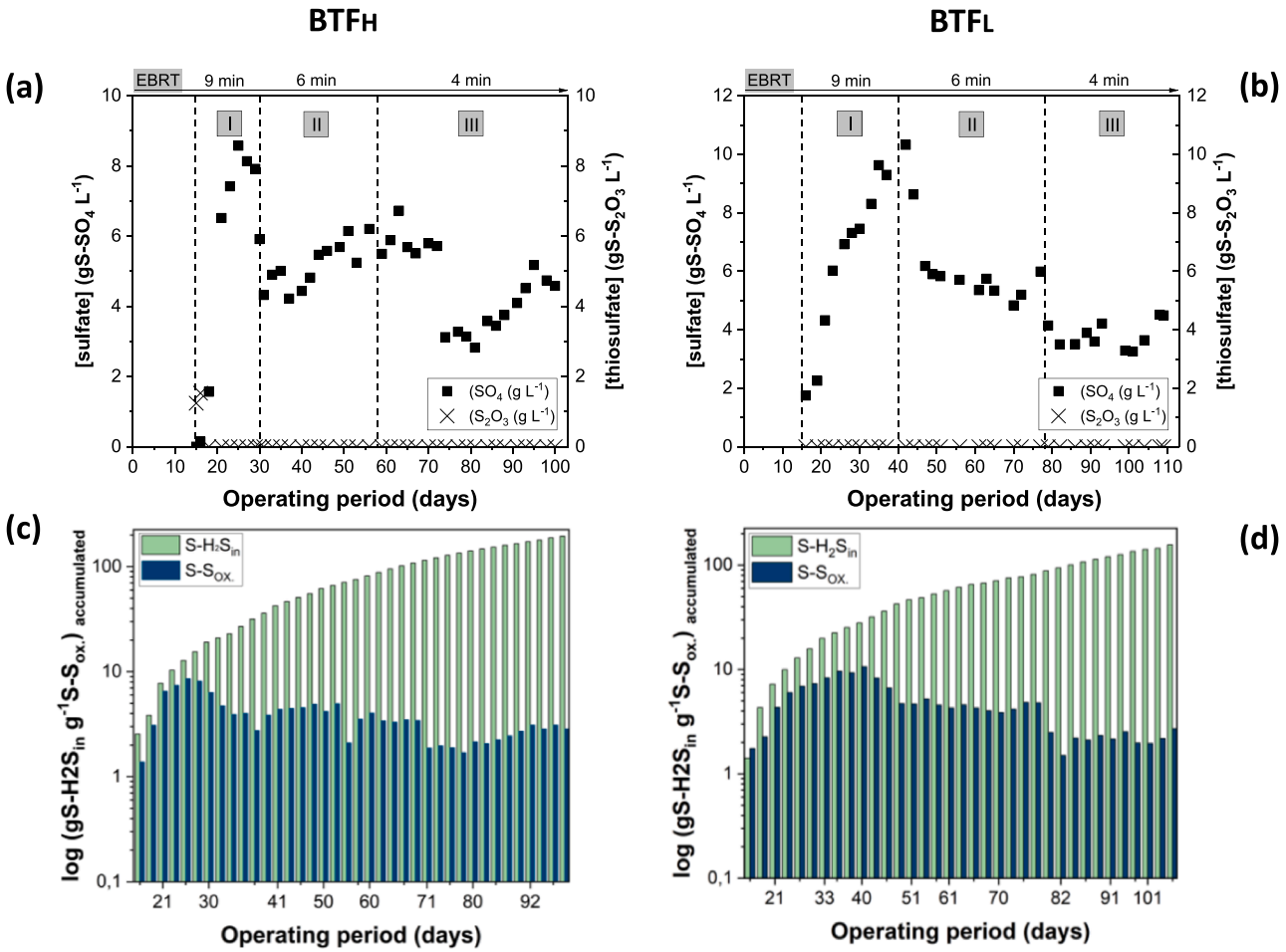

Fig. 6. Time course of cumulative sulfur oxidized species ($S_{ox.}$) in the aqueous phase (SO_4, S_2O_3) related to the total cumulative inlet gaseous H_2S (H_2S_{in}).

operational stability.

On an industrial scale, oxygen (or air) is typically injected into the H_2S-laden stream before entering the BTF [6]. As a result, significant quantities of air are required to supply enough oxygen for the complete biological conversion of H_2S to sulfate. However, the high operational costs of running the blower, combined with the dilution of biogas (entailing a decrease in the gas-liquid concentration gradients), can negatively impact the economic feasibility of the process due to limitations in mass transfer between the gas and liquid phases [26]. Therefore, it is essential to explore alternative technologies or optimization strategies to mitigate these challenges and enhance the efficiency and economic sustainability of the process. Since gas dilution is not a concern in fermentative systems, an efficient hybrid aerobic-anoxic biodesulfurization system applied to high sulfur streams, as proposed in this study (7000 ppm_v H_2S), can help mitigating clogging issues and improving mass transfer efficiency by optimizing oxygen utilization in sugarcane biorefineries. Indeed, by integrating aerobic and anoxic zones, the biological conversion of H_2S to either sulfate or elemental sulfur can be optimized, while minimizing the need for excess air and maintaining a more concentrated biogas flow. According to Cano et al. [15], the cost of nitrate per kilogram of sulfur-treated H_2S accounted for 0.54€ at a N/S ratio of 0.4 mol mol^{-1}, which is similar to the ratio applied in this system. On the other hand, increasing the N/S ratio to 1.6 mol mol^{-1} could reduce sulfur production to nearly negligible levels, although it would result in a higher nitrate cost of €2.15 per kg of sulfur-treated. operational expenses such as energy consumption, labor, and maintenance or re-setup costs due to clogging. However, costs associated with reactor restart due to clogging events were not explicitly addressed by the authors.

Alternatively, nitrate supplementation could be sourced from ammonium-rich wastewater streams (e.g. i.e., swine wastewater, slurry from rural household anaerobic digesters, domestic sewage from primary sedimentation tanks, landfill leachate, pig slurry), thus reducing nitrate consumption [96,3,52,72,84,86]. From these studies, a nitrifying tank would be required to allow full or partial nitrification, with the choice depending on whether nitrate or nitrite is used, as this influences whether sulfate or elemental sulfur is produced. Partial nitrification to nitrite can be advantageous in scenarios with high ammonia concentrations, as it requires less aeration and thus lower OPEX, though it involves more complex control due to higher nitrogen demand for H_2S oxidation. However, the use of nitrate and carbon-rich wastewater in BTFs introduces the potential for heterotrophic bacterial growth, which could impact H_2S removal efficiency. Heterotrophic bacteria, thriving in environments rich in organic carbon, may outcompete autotrophic SOB for resources like nitrate, as observed by Khanongnuch et al. [44]. This competitive dynamic can lead to increased biomass production, exacerbating clogging and causing pressure drops in the packed bed, which compromises the system's operational stability. Conversely, the presence of heterotrophic bacteria might foster synergistic interactions within the microbial community, potentially enhancing overall system performance. The robustness of simultaneous biogas desulfurization and nitrogen removal has been demonstrated with various ammonium-rich effluents and bioreactor configurations [23,39,92,95,96], underscoring the need to tailor each system to specific biogas characteristics and effluent properties. Further laboratory-scale research, pilot studies, and industrial-scale implementations are crucial for accurately assessing operational costs, installation expenses, and environmental impacts. Long-term studies are essential to evaluate the effects of seasonal

variations in effluent composition, with robust control systems playing a critical role in mitigating external disturbances and maintaining stable operation. Moreover, further studies should focus on the assessment of a wider range of N/S ratios in anoxic-aerobic BTFs to provide deeper insights into the fate of H_2S.

4. Conclusions

The BTFs achieved complete H_2S removal with a maximum EC of 160 gS-H_2S $m^{-}3h^{-1}$ and sustained removal efficiencies at inlet concentrations of 7000 ppm_v H_2S. This study demonstrated that packing material properties are pivotal for system performance, with the Kaldnes K1 Micro rings in BTF_H showing enhanced mass transfer but rapid clogging due to sulfur accumulation, highlighting the need for balancing surface area and operational conditions. In contrast, BTF_L, using polyhedral hollow balls, provided greater stability due to a lower propensity for clogging. The integration of aerobic and anoxic zones improved sulfur oxidation control, optimizing N/S molar ratios, and reducing the need for excess air injection. This hybrid system design advances sustainable biogas desulfurization, particularly for sugarcane biorefineries, by enabling the use of low-cost nitrate sources, such as ammonium-rich wastewater. Future studies should expand on N/S ratio optimization and pilot-scale studies to fine-tune the economic and environmental performance of aerobic-anoxic biofilters for broader industrial adoption.

Environmental Implications

This work presents a novel hybrid aerobic-anoxic biotrickling filtration (BTF) system tailored to address the critical environmental and operational challenges associated with the removal of high hydrogen sulfide (H_2S) concentrations generated during sugarcane vinasse fermentation. Understanding biological desulfurization in high-H_2S streams is pivotal for mitigating multiple challenges in industrial operations. In sugarcane biorefineries, efficient H_2S management reduces sulfur emissions that harm the environment and human health, while tackling operational issues such as corrosion and equipment degradation. Moreover, mastering these processes creates opportunities to recover valuable biomass and nutrients, enhancing both the sustainability and economic viability of biorefineries.

CRediT authorship contribution statement

Raul Munoz: Writing – review & editing, Supervision, Project administration, Funding acquisition, Data curation, Conceptualization; **Márcia Helena Rissato Zamariolli Damianovic:** Writing – review & editing, Project administration, Funding acquisition, Data curation, Conceptualization; **André do Vale Borges:** Writing – original draft, Software, Methodology, Investigation, Conceptualization.

Declaration of Competing Interest

The authors declare that they have no known competing financial interests or personal relationships that could have appeared to influence the work reported in this paper.

Acknowledgments

This work was supported by the São Paulo Research Foundation [grant numbers 2021/15245-5; 2023/04885-9]. The authors also acknowledge the regional government of Castilla y León (UIC 379).

Appendix A. Supporting information

Supplementary data associated with this article can be found in the online version at doi:10.1016/j.jhazmat.2025.137696.

Data Availability

Data will be made available on request.

References

[1] Adekunle, K.F., Okolie, J.A., 2015. A review of biochemical process of anaerobic digestion. Adv Biosci Bioeng 6 (3), 205–212. https://doi.org/10.4236/abb.2015.63020.
[2] Alayande, A.B., Jee, H., Kang, D., Jang, J.K., Chae, K.-J., Hwang, M.-H., et al., 2024. Membrane and adsorption technologies for efficient hydrogen sulfide removal from biogas: a review focused on the advancement of key components. Process Saf Environ Prot 186, 448–473. https://doi.org/10.1016/j.psep.2024.04.018.
[3] Almenglo, F., Bezerra, T., Lafuente, J., Gabriel, D., Ramírez, M., Cantero, D., 2016. Effect of gas-liquid flow pattern and microbial diversity analysis of a pilot-scale biotrickling filter for anoxic biogas desulfurization. Chemosphere 157, 215–223. https://doi.org/10.1016/j.chemosphere.2016.05.016.
[4] Almenglo, F., González-Cortés, J.J., Ramírez, M., Cantero, D., 2023. Recent advances in biological technologies for anoxic biogas desulfurization. Chemosphere 321, 138084. https://doi.org/10.1016/j.chemosphere.2023.138084.
[5] APHA, AWWA, WEF, 2012 Standard methods for examination of water and wastewater. 22 nd. ed., APHA. Washington, D.C.
[6] Ariman, S., Koyuncu, S., 2022. Removal of hydrogen sulfide in biogas from wastewater treatment sludge by real scale biotrickling filtration desulfurization process. Water Pract Technol 17 (7), 1406–1420. https://doi.org/10.2166/wpt.2022.072.
[7] Azizi, S.M.M., Zakaria, B.S., Haffiez, N., Niknejad, P., Dhar, B.R., 2022. A critical review of prospects and operational challenges of microaeration and iron dosing for in-situ biogas desulfurization. Bioresour Technol Rep 20, 101265. https://doi.org/10.1016/j.biteb.2022.101265.
[8] Barbusinski, K., Kalemba, K., Kasperczyk, D., Urbaniec, K., Kozik, V., 2017. Biological methods for odor treatment – a review. J Clean Prod 152, 223–241. https://doi.org/10.1016/j.jclepro.2017.03.093.
[9] Bayrakdar, A., Tilahun, E., Calli, B., 2016. Biogas desulfurization using autotrophic denitrification process. Appl Microbiol Biotechnol 100, 939–948. https://doi.org/10.1007/s00253-015-7017-z.
[10] Borges, A.V., Fuess, L.T., Alves, L.T., Takeda, I., Damianovic, P.Y., 2021. M.H.R.Z. Co-digesting sugarcane vinasse and distilled glycerol to enhance bioenergy generation in biofuel-producing plants. Energy Convers Manag 250, 114897. https://doi.org/10.1016/j.enconman.2021.114897.
[11] Borges, A.V., Fuess, L.T., Takeda, L.T., Alves, P.Y., Dias, I., Damianovic, M.E.S., 2022. M.H.R.Z. Co-digestion of biofuel by-products: enhanced biofilm formation maintains high organic matter removal when methanogenesis fails. J Environ Manag 310, 114768. https://doi.org/10.1016/j.jenvman.2022.114768.
[12] Borges, A.V., Fuess, L.T., Takeda, P.Y., Rogeri, R.C., Saia, F.T., Gregoracci, G.B., et al., 2025. Unleashing the full potential of vinasse fermentation in sugarcane biorefineries. Renew Sustain Energy Rev 208, 115096. https://doi.org/10.1016/j.rser.2024.115096.
[13] Brito, J., Valle, A., Almenglo, F., Ramírez, M., Cantero, D., 2018. Progressive change from nitrate to nitrite as the electron acceptor for the oxidation of H2S under feedback control in an anoxic biotrickling filter. Biochem Eng J 139, 154–161. https://doi.org/10.1016/j.bej.2018.08.017.
[14] Bu, H., Carvalho, G., Huang, C., Sharma, K.R., Yuan, Z., Song, Y., et al., 2022. Evaluation of continuous and intermittent trickling strategies for the removal of hydrogen sulfide in a biotrickling filter. Chemosphere 291 (Part 1), 132723. https://doi.org/10.1016/j.chemosphere.2021.132723.
[15] Cano, P.I., Brito, J., Almenglo, F., Ramírez, M., Gomez, J.M., Cantero, D., 2019. Influence of trickling liquid velocity, low molar ratio of nitrogen/sulfur and gas-liquid flow pattern in anoxic biotrickling filters for biogas desulfurization. Biochem Eng J 148, 205–213. https://doi.org/10.1016/j.bej.2019.05.008.
[16] Cano, P.I., Colon, J., Ramirez, M., Lafuente, J., Gabriel, D., Cantero, D., 2018. Life cycle assessment of different physical-chemical and biological technologies for biogas desulfurization in sewage treatment plants. J Clean Prod 181, 663–674. https://doi.org/10.1016/j.jclepro.2018.02.018.
[17] Cattaneo, C.R., Muñoz, R., Korshin, G.V., Naddeo, V., Belgiorno, V., Zarra, T., 2023. Biological desulfurization of biogas: a comprehensive review on sulfide microbial metabolism and treatment biotechnologies. Sci Total Environ 893, 164689. https://doi.org/10.1016/j.scitotenv.2023.164689.
[18] Chung, Y.C., 2007. Evaluation of gas removal and bacterial community diversity in a biofilter developed to treat composting exhaust gases. J Hazard Mater 144 (1-2), 377–385. https://doi.org/10.1016/j.jhazmat.2006.10.045.
[19] Chung, Y.C., Huang, C., Tseng, C.P., 1996. Operation optimization of *Thiobacillus thioparus CH11* biofilter for hydrogen sulfide removal. J Biotechnol 52 (1), 31–38. https://doi.org/10.1016/S0168-1656(96)01622-7.
[20] Costanzo, N.D., Di Capua, F., Cesaro, A., Carraturo, F., Salamone, M., Guida, M., et al., 2024. Headspace micro-oxygenation as a strategy for efficient biogas desulfurization and biomethane generation in a centralized sewage sludge digestion plant. Biomass– Bioenergy 183, 107151. https://doi.org/10.1016/j.biombioe.2024.107151.
[21] Cox, H.H.J., Deshusses, M.A., Converse, B.M., Schroeder, E.D., Iranpour, R., 2002. Odor and volatile organic compound treatment by biotrickling filters: pilot-scale

studies at hyperion treatment plant. Water Environ Res 74 (6), 557–563. https://doi.org/10.2175/106143002x140369.
[22] Dada, O.I., Yu, L., Neibergs, S., Chen, S., 2025. Biodesulfurization: effective and sustainable technologies for biogas hydrogen sulfide removal. Renew Sustain Energy Rev 209, 115144. https://doi.org/10.1016/j.rser.2024.115144.
[23] Deng, L., Chen, H., Chen, Z., Liu, Y., Pu, X., Song, L., 2009. Process of simultaneous hydrogen sulfide removal from biogas and nitrogen removal from swine wastewater. Bioresour Technol 100 (23), 5600–5608. https://doi.org/10.1016/j.biortech.2009.06.012.
[24] Deng, T., He, Z., Xu, M., Dong, M., Guo, J., Sun, G., et al., 2023. Species' functional traits and interactions drive nitrate-mediated sulfur-oxidizing community structure and functioning. mBio 14 (5), e0156723. https://doi.org/10.1128/mbio.01567-23.
[25] Dias, M.E.S., Takeda, P.Y., Fuess, L.T., Tommaso, G., 2023. Inoculum-to-substrate ratio and solid content effects over in natura spent coffee grounds anaerobic digestion. J Environ Manag 325 (Part B), 116486. https://doi.org/10.1016/j.jenvman.2022.116486.
[26] Dobslaw, D., Ortlinghaus, O., 2020. Biological waste air and waste gas treatment: overview, challenges, operational efficiency, and current trends. Sustainability 12 (20), 8577. https://doi.org/10.3390/su12208577.
[27] Duan, H., Koe, L.C., Yan, R., Chen, X., 2006. Biological treatment of H_2S using pellet activated carbon as a carrier of microorganisms in a biofilter. Water Res 40 (14), 2629–2636. https://doi.org/10.1016/j.watres.2006.05.021.
[28] Ezechi, E.E., Kutty, S.R.B.M., Isa, M.H., Malakahmad, Ude, A.C.M., Menyechi, E. J., et al., 2015. Nutrient removal from wastewater by integrated attached growth bioreactor. Res J Environ Toxicol 10, 28–38.
[29] Fernández, M., Ramírez, M., Gómez, J.M., Cantero, D., 2014. Biogas biodesulfurization in an anoxic biotrickling filter packed with open-pore polyurethane foam. J Hazard Mater 264, 529–535. https://doi.org/10.1016/j.jhazmat.2013.10.046.
[30] Fernández, M., Ramírez, M., Pérez, R.M., Gómezm, J.M., Cantero, D., 2013. Hydrogen sulphide removal from biogas by an anoxic biotrickling filter packed with Pall rings. Chemical Engineering Journal 225, 456–463. https://doi.org/10.1016/j.cej.2013.04.020.
[31] Fortuny, M., Baeza, J.A., Gamisans, X., Casas, C., Lafuente, J., Deshusses, M.A., et al., 2008. Biological sweetening of energy gases mimics in biotrickling filters. Chemosphere 71 (1), 10–17. https://doi.org/10.1016/j.chemosphere.2007.10.072.
[32] Fortuny, M., Guisasola, A., Casas, C., Gamisans, X., Lafuente, J., Gabriel, D., 2010. Oxidation of biologically produced elemental sulfur under neutrophilic conditions. Wiley Intersci 85 (3), 378–386. https://doi.org/10.1002/jctb.2333.
[33] Fuess, L.T., Braga, A.F.M., Eng, F., Gregoracci, G.B., Saia, F.T., Zaiat, M., et al., 2023. Solving the bottlenecks of sugarcane vinasse biodigestion: Impacts of temperature and substrate exchange on sulfate removal during dark fermentation. Chem Eng J 455 (Part 2). https://doi.org/10.1016/j.cej.2022.140965.
[34] Fuess, L.T., De Araújo Júnior, M.M., Garcia, M.L., Zaiat, M., 2017. Designing full-scale biodigestion plants for the treatment of vinasse in sugarcane biorefineries: How phase separation and alkalinization impact biogas and electricity production costs? Chem Eng Res Des 119, 209–220. https://doi.org/10.1016/j.cherd.2017.01.023.
[35] Fuess, L.T., Kiyuna, L.S.M., Ferraz Júnior, A.D., Persinoti, G.F., Squina, F.M., GArcia, M.L., et al., 2017. Thermophilic two-phase anaerobic digestion using an innovative fixed-bed reactor for enhanced organic matter removal and bioenergy recovery from sugarcane vinasse. Appl Energy 189, 480–491. https://doi.org/10.1016/j.apenergy.2016.12.071.
[36] Fuess, L.T., Rogeri, R.G., Eng, F., Borges, A.V., Winkler, P.B., Etchebehere, C., et al., 2024. Thermophilic fermentation of sugarcane vinasse: Process flexibility explained through characterizing microbial community and predicting metabolic functions. Int J Hydrog Energy 77, 1339–1351. https://doi.org/10.1016/j.ijhydene.2024.06.200.
[37] Gabriel, D., Deshusses, M.A., 2003. Performance of a full-scale biotrickling filter treating H2S at a gas contact time of 1.6 to 2.2 seconds. Environ Prog 22, 111–118. https://doi.org/10.1002/ep.670220213.
[38] González-Cortés, J.J., Almenglo, F., Ramírez, M., Cantero, D., 2021. Simultaneous removal of ammonium from landfill leachate and hydrogen sulfide from biogas using a novel two-stage oxic-anoxic system. Sci Total Environ 750, 11. https://doi.org/10.1016/j.scitotenv.2020.141664.
[39] González-Cortés, J.J., Torres-Herrera, S., Almenglo, F., Ramírez, M., Cantero, D., 2021. Anoxic biogas biodesulfurization promoting elemental sulfur production in a Continuous Stirred Tank Bioreactor. J Hazard Mater 401, 10 https://doi.org/10.1016/j. jhazmat.2020.123785.
[40] Jaber, M.B., Couvert, A., Amrane, A., Le Cloirec, P., Dumont, E., 2017. Hydrogen sulfide removal from a biogas mimic by biofiltration under anoxic conditions. J Environ Chem Eng 5 (6), 5617–5623. https://doi.org/10.1016/j.jece.2017.10.029.
[41] Jia, T., Sun, S., Zhao, Q., Peng, Y., Zhang, L., 2022. Extremely acidic condition (pH<1.0) as a novel strategy to achieve high-efficient hydrogen sulfide removal in biotrickling filter: Biomass accumulation, sulfur oxidation pathway and microbial analysis. Chemosphere 294, 133770. https://doi.org/10.1016/j.chemosphere.2022.133770.
[42] Jung, H., Kim, D., Choi, H., Lee, C., 2022. A review of technologies for in-situ sulfide control in anaerobic digestion. Renew Sustain Energy Rev 157, 112068. https://doi.org/10.1016/j.rser.2021.112068.
[43] Juntranapaporn, J., Vikromvarasiri, N., Soralump, C., Pisutpaisal, N., 2019. Hydrogen sulfide removal from biogas in biotrickling filter system inoculated with *Paracoccus pantotrophus*. Int J Hydrog Energy 44 (56), 29554–29560. https://doi.org/10.1016/j.ijhydene.2019.03.069.
[44] Khanongnuch, R., Di Capua, F., Lakaniemi, A.M., Rene, E.R., Lens, P.N., 2019. Transient–state operation of an anoxic biotrickling filter for H_2S removal. J Hazard Mater 377, 42–51. https://doi.org/10.1016/j.jhazmat.2019.05.043.
[45] Khoshnevisan, B., Tsapekos, P., Alfaro, N., Diaz, I., Polanco, M.F., Rafiee, S., et al., 2017. A review on prospects and challenges of biological H_2S removal from biogas with focus on biotrickling filtration and microaerobic desulfurization. Biofuel Res J 16, 741–750. https://doi.org/10.18331/BRJ2016.4.4.6.
[46] Kim, S., Deshusses, M.A., 2005. Understanding the limits of H_2S degrading biotrickling filters using a differential biotrickling filter. Chem Eng J 113 (2–3), 119–126. https://doi.org/10.1016/j.cej.2005.05.001.
[47] Kim, J.H., Rene, E.R., Park, H.S., 2008. Biological oxidation of hydrogen sulfide under steady and transient state conditions in an immobilized cell biofilter. Bioresour Technol 99 (3), 583–588. https://doi.org/10.1016/j.biortech.2006.12.028.
[48] Latifi, P., Karrabi, M., Danesh, S., 2019. Anaerobic co-digestion of poultry slaughterhouse wastes with sewage sludge in batch-mode bioreactors (effect of inoculum-substrate ratio and total solids). Renew Sustain Energy Rev 107, 288–296. https://doi.org/10.1016/j.rser.2019.03.015.
[49] Lebrero, R., Toledo-Cervantes, A., Muñoz, R., Del Nery, V., Foresti, E., 2016. Biogas upgrading from vinasse digesters: a comparison between an anoxic biotrickling filter and an algal-bacterial photobioreactor. J Chem Technol Biotechnol 91, 2488–2495. https://doi.org/10.1002/jctb.4843.
[50] Lee, S.H., Kurade, M.B., Jeon, B.H., Kim, J., Zheng, Y., Salama, E.S., 2021. Water condition in biotrickling filtration for the efficient removal of gaseous contaminants. Crit Rev Biotechnol 41 (8), 1279–1296. https://doi.org/10.1080/07388551.2021.1917506.
[51] Lee, D.-J., Wong, B.-T., 2014. Denitrifying sulfide removal and nitrososulfide complex: Azoarcus sp. NSC3 and Pseudomonas sp. CRS1 mix. Bioresour Technol 166, 616–619. https://doi.org/10.1016/j.biortech.2014.05.099.
[52] Lenis, A., Ramírez, M., González-Cortés, J.J., Ooms, K., Pinnekamp, J., 2023. Implementation of a pilot-scale biotrickling filtration process for biogas desulfurization under anoxic conditions using agricultural digestate as trickling liquid. Bioengineering 10 (2), 160. https://doi.org/10.3390/bioengineering10020160.
[53] Li, X., Jiang, X., Zhou, Q., et al., 2016. Effect of S/N Ratio on the Removal of Hydrogen Sulfide from Biogas in Anoxic Bioreactors. Appl Biochem Biotechnol 180, 930–944. https://doi.org/10.1007/s12010-016-2143-3.
[54] Lin, S., Mackey, H.R., Hao, T., Guo, G., Van Loosdrecht, M.C.M., Chen, G., 2018. Biological sulfur oxidation in wastewater treatment: a review of emerging opportunities. Water Res 143, 399–415. https://doi.org/10.1016/j.watres.2018.06.051.
[55] Liu, S., Gao, P.F., Li, S., Fu, H., Wang, L., Dai, Y., et al., 2023. A review of the recent progress in biotrickling filters: packing materials, gases, micro-organisms, and CFD. Environ Sci Pollut Res 30, 125398–125416. https://doi.org/10.1007/s11356-023-31004-7.
[56] López, L.R., Bezerra, T., Mora, M., Lafuente, J.A.N.D., Gabriel, D., 2015. Influence of trickling liquid velocity and flow pattern in the improvement of oxygen transport in aerobic biotrickling filters for biogas desulfurization. J Chem Technol Biotechnol 91, 1031–1039. https://doi.org/10.1002/jctb.4676.
[57] Mari, A.G., Andreani, C.L., Tonello, T.U., Leite, L.C.C., Fernandes, J.R., Lopes, D. D., et al., 2020. Biohydrogen and biomethane production from cassava wastewater in a two-stage anaerobic sequencing batch biofilm reactor. Int J Hydrog Energy 45 (8), 5165–5174. https://doi.org/10.1016/j ijhydene.2019.07.054.
[58] Meier, T.R.W., Cremonez, P.A., Maniglia, T.C., Sampaio, S.C., Teleken, J.G., Silva, E.A., 2020. Production of biohydrogen by an anaerobic digestion process using the residual glycerol from biodiesel production as an additive to cassava wastewater. J Clean Prod 258, 120833. https://doi.org/10.1016/j.jclepro.2020.120833.
[59] Méndez, L., García, D., Perez, E., Blanco, S., Muñoz, R., 2022. Photosynthetic upgrading of biogas from anaerobic digestion of mixed sludge in an outdoors algal-bacterial photobioreactor. J Water Process Eng 48, 102891. https://doi.org/10.1016/j.jwpe.2022.102891.
[60] Mol, A.R., Pruim, S.D., De Korte, M., Meuwissen, D.J.M., Van Der Weijden, R.D., Klok, J.B.M., et al., 2022. Removal of small elemental sulfur particles by polysulfide formation in a sulfidic reactor. Water Res 227, 119296. https://doi.org/10.1016/j.watres.2022.119296.
[61] Montebello, A.M., Baeza, M., Lafuente, J., Gabriel, D., 2010. Monitoring and performance of a desulphurizing biotrickling filter with an integrated continuous gas/liquid flow analyzer. Chem Eng J 165 (2), 500–507. https://doi.org/10.1016/j.cej.2010.09.053.
[62] Montebello, A.M., Bezerra, T., Rovira, R., Rago, L., Lafuente, J., Gamisans, X., et al., 2013. Operational aspects, pH transition and microbial shifts of a H_2S desulfurizing biotrickling filter with random packing material. Chemosphere 93 (11), 2675–2682. https://doi.org/10.1016/j.chemosphere.2013.08.
[63] Montebello, A., Fernández, M., Almenglo, F., Ramírez, M., Cantero, D., Baeza, M., et al., 2012. Simultaneous methylmercaptan and hydrogen sulfide removal in the desulfurization of biogas in aerobic and anoxic biotrickling filters. Chem Eng J 200–202, 237–246. https://doi.org/10.1016/j.cej.2012.06.043.
[64] Montebello, A.M., Mora, M., López, L.R., Bezerra, T., Gamisans, X., Lafuente, J., et al., 2014. Aerobic desulfurization of biogas by acidic biotrickling filtration in a randomly packed reactor. J Hazard Mater 280, 200–208. https://doi.org/10.1016/j.jhazmat.2014.07.075.

[65] Muñoz, R., Meier, L., Diaz, I., Jeison, D., 2015. A review on the state-of-the-art of physical/chemical and biological technologies for biogas upgrading. Rev Environ Sci Biotechnol 14, 727–759. https://doi.org/10.1007/s11157-015-9379-1.
[66] Nhut, H.H., Thanh, V.L.T., Le, L.T. Removal of H_2S in biogas using biotrickling filter: recent development. Process Saf Environ Protect, 144, 297-309,
[67] Nisola, G.M., Tuuguu, E., Farnazo, D.M., Han, M., Kim, Y., Cho, E., et al., 2010. Hydrogen sulfide degradation characteristics of Bordetella sp. Sulf-8 in a biotrickling filter. Bioprocess Biosyst Eng 33 (9), 1131–1138. https://doi.org/10.1007/s00449-010-0440-8.
[68] Omri, I., Bouallagui, H., Aouidi, F., Godon, J.-J., Hamdi, M., 2011. H_2S gas biological removal efficiency and bacterial community diversity in biofilter treating wastewater odor. Bioresour Technol 102 (22), 10202–10209. https://doi.org/10.1016/j.biortech.2011.05.094.
[69] Pachiega, R., Rodrigues, M.F., Rodrigues, C.V., Sakamoto, I.K., Varesche, M.B., De Oliveira, J.E., et al., 2019. Hydrogen bioproduction with anaerobic bacteria consortium from brewery wastewater. Int J Hydrog Energy 44 (1), 155–163. https://doi.org/10.1016/j.ijhydene.2018.02.107.
[70] Pascual, C., Cantera, S., Muñoz, R., Lebrero, R., 2020. Comparative assessment of two biotrickling filters for siloxanes removal: Effect of the addition of an organic phase. Chemosphere 251, 126359. https://doi.org/10.1016/j.chemosphere.2020.126359.
[71] Piffer, M.A., Zaiat, M., Nascimento, C.A.O., Fuess, L.T., 2021. Dynamics of sulfate reduction in the thermophilic dark fermentation of sugarcane vinasse: a biohydrogen-independent approach targeting enhanced bioenergy production. J Environ Chem Eng 9 (5). https://doi.org/10.1016/j.jece.2021.105956.
[72] Pirolli, M., Da Silva, M.L.B., Mezzari, M.P., Michelon, W., Prandini, J.M., Soares, H.M., 2016. Methane production from a field-scale biofilter designed for desulfurization of biogas stream. J Environ Manag 177, 161–168. https://doi.org/10.1016/j.jenvman.2016.04.013.
[73] Pudi, A., Rezaei, M., Signorini, V., Andersson, M.P., Baschetti, M.G., Mansouri, S. S., 2022. Hydrogen sulfide capture and removal technologies: a comprehensive review of recent developments and emerging trends. Sep Purif Technol 298, 121448. https://doi.org/10.1016/j.seppur.2022.121448.
[74] Qiu, X., Deshusses, M.A., 2017. Performance of a monolith biotrickling filter treating high concentrations of H_2S from mimic biogas and elemental sulfur plugging control using pigging. Chemosphere 186, 790–797. https://doi.org/10.1016/j.chemosphere.2017.08.032.
[75] Ramirez, M., Gomez, J.M., Aroca, G., Cantero, D., 2009. Removal of hydrogen sulfide and ammonia from gas mixtures by co-immobilized cells using a new configuration of two biotrickling filters. Water Sci Technol 59 (7), 1353–1359. https://doi.org/10.2166/wst.2009.105.
[76] Ramos, I., Pérez, R., Fdz-Polanco, M., 2013. Microaerobic desulphurization unit: a new biological system for the removal of H2S from biogas. Bioresour Technol 142, 633–640. https://doi.org/10.1016/j.biortech.2013.05.08.
[77] Reddy, C.N., Bae, S., Min, B., 2019. Biological removal of H_2S gas in a semi-pilot scale biotrickling filter: optimization of various parameters for efficient removal at high loading rates and low pH conditions. Bioresour Technol 285, 121328. https://doi.org/10.1016/j.biortech.2019.121328.
[78] Rodriguez, G., Dorado, A.D., Fortuny, M., Gabriel, D., Gamisans, X., 2014. Biotrickling filters for biogas sweetening: oxygen transfer improvement for a reliable operation. Process Saf Environ Prot 92 (3), 261–268. https://doi.org/10.1016/j.psep.2013.02.002.
[79] Rogeri, R.C., Fuess, L.T., Araujo, D.E., Eng, M.N., Borges, F., Damianovic, A.V., et al., 2024. A.J. Methane production from sugarcane vinasse: the alkalinizing potential of fermentative-sulfidogenic processes in two-stage anaerobic digestion. Energy Nexus 14, 100303. https://doi.org/10.1016/j.nexus.2024.100303.
[80] Rogeri, R.C., Fuess, L.T., Eng, F., Borges, A.V., Araujo, M.N., Damianovic, M.H.R. Z., et al., 2023. Strategies to control pH in the dark fermentation of sugarcane vinasse: Impacts on sulfate reduction, biohydrogen production and metabolite distribution. J Environ Manag 325 (Part B). https://doi.org/10.1016/j.jenvman.2022.116495.
[81] Sáez-Orviz, S., Lebrero, R., Terrén, L., Doñate, S., Esclapez, M.D., Saúco, L., et al., 2024. Evaluation of the performance of new plastic packing materials from plastic waste in biotrickling filters for odor removal. Process Saf Environ Prot 191 (Part B), 2361–2372. https://doi.org/10.1016/j.psep.2024.10.009.
[82] Sakarika, M., Stavropoulos, K., Kopsahelis, A., Koutra, E., Zafiri, C., Kornaros, M., 2020. Two-stage anaerobic digestion harnesses more energy from the co-digestion of end-of-life dairy products with agro-industrial waste compared to the single-stage process. Biochem Eng J 153, 107404. https://doi.org/10.1016/j.bej.2019.107404.
[83] Scarcelli, P.G., Ruas, G., Lopez-Serna, R., Serejo, M.L., Blanco, S., Boncz, M.A., et al., 2021. Integration of algae-based sewage treatment with anaerobic digestion of the bacterial-algal biomass and biogas upgrading. Bioresour Technol 340, 125552. https://doi.org/10.1016/j.biortech.2021.125552.
[84] Sekine, M., Akizuki, S., Kishi, M., Kurosawa, N., Toda, T., 2020. Simultaneous biological nitrification and desulfurization treatment of ammonium and sulfide-rich wastewater: effectiveness of a sequential batch operation. Chemosphere 244, 125381. https://doi.org/10.1016/j.chemosphere.2019.125381.
[85] Severi, C.A., Pascual, C., Perez, V., Muñoz, R., Lebrero, R., 2025. Pilot-scale biogas desulfurization through anoxic biofiltration. J Hazard Mater, 136830. https://doi.org/10.1016/j.jhazmat.2024.136830.
[86] Soreanu, G., Béland, M., Falletta, P., Edmonson, K., Seto, P., 2008. Laboratory pilot scale study for H_2S removal from biogas in an anoxic biotrickling filter. Water Sci Technol 57 (2), 201–207. https://doi.org/10.2166/wst.2008.023.
[87] Struk, M., Sepúlveda-Muñoz, C.A., Kushkevych, I., Muñoz, 2023. Photoautotrophic removal of hydrogen sulfide from biogas using purple and green sulfur bacteria. J Hazard Mater 443 (Part B), 130337. https://doi.org/10.1016/j.jhazmat.2022.130337.
[88] Sun, Z., Cheng, Z., Wang, J., Kennes, C., Chen, D., Yu, J., et al., 2024. Fe (II)/Fe (III) regulated adaptive biofilm responses and microbial metabolic mechanisms for enhanced cycloalkane biodegradation. Chem Eng J 500, 157388. https://doi.org/10.1016/j.cej.2024.157388.
[89] Tanikawa, D., Fujise, R., Kondo, Y., Fujihira, T., Seo, S., 2018. Elimination of hydrogen sulfide from biogas by a two-stage trickling filter system using effluent from anaerobic–aerobic wastewater treatment. Int Biodeterior Biodegrad 130, 98–101. https://doi.org/10.1016/j.ibiod.2018.04.007.
[90] Ucar, D., Yilmaz, T., Di Capua, F., Esposito, G., Sahinkaya, E., 2020. Comparison of biogenic and chemical sulfur as electron donors for autotrophic denitrification in sulfur-fed membrane bioreactor (SMBR). Bioresour Technol 299, 122574. https://doi.org/10.1016/j.biortech.2019.122574.
[91] Vikromvarasiri, N., Champreda, V., Boonyawanich, S., Pisutpaisal, N., 2017. Hydrogen sulfide removal from biogas by biotrickling filter inoculated with *Halothiobacillus neapolitanus*. Int J Hydrog Energy 42 (29), 18425–18433. https://doi.org/10.1016/j.ijhydene.2017.05.020.
[92] Wang, L., Wei, B., Chen, Z., Deng, L., Song, L., Wang, S., et al., 2015. Effect of inoculum and sulfide type on simultaneous hydrogen sulfide removal from biogas and nitrogen removal from swine slurry and microbial mechanism. Appl Microbiol Biotechnol 99, 10793–10803. https://doi.org/10.1007/s00253-015-6916-3.
[93] Werkneh, A.A., 2022. Biogas impurities: environmental and health implications, removal technologies and future perspectives. Heliyon 8 (10). https://doi.org/10.1016/j.heliyon.2022.e10929.
[94] Wu, J., Jiang, X., Jin, Z., Yang, S., Zhang, J., 2020. The performance and microbial community in a slightly alkaline biotrickling filter for the removal of high concentration H_2S from biogas. Chemosphere 249, 126127. https://doi.org/10.1016/j.chemosphere.2020.12.
[95] Xu, X.J., Li, H.J., Wang, W., Zhang, R.C., Zhou, X., Xing, D.F., et al., 2020. The performance of simultaneous denitrification and biogas desulfurization system for the treatment of domestic sewage. Chem Eng J 399, 125855. https://doi.org/10.1016/j.cej.2020.125855.
[96] Zeng, Y., Luo, Y., Huan, C., Shuai, Y., Liu, Y., Xu, L., et al., 2019. Anoxic biodesulfurization using biogas digestion slurry in biotrickling filters. J Clean Prod 224, 88–99. https://doi.org/10.1016/j.jclepro.2019.03.218.
[97] Zeng, Y., Xiao, L., Zhang, X., Zhou, J., Ji, G., Schroeder, S., et al., 2018. Biogas desulfurization under anoxic conditions using synthetic wastewater and biogas slurry. Int Biodeterior Biodegrad 133, 247–255. https://doi.org/10.1016/j.ibiod.2018.05.012.
[98] Zhang, Y., Oshita, K., Kusakabe, T., Takaoka, M., Kawasaki, Y., Minami, D., et al., 2020. Simultaneous removal of siloxanes and H_2S from biogas using an aerobic biotrickling filter. J Hazard Mater 391, 122187. https://doi.org/10.1016/j.jhazmat.2020.122187.
[99] Zhang, Y., Oshita, K., Takaoka, M., Kawasaki, Y., Minami, D., Inoue, G., et al., 2021. Effect of pH on the performance of an acidic biotrickling filter for simultaneous removal of H_2S and siloxane from biogas. Water Sci Technol 83 (7), 1511–1521. https://doi.org/10.2166/wst.2021.083.
[100] Zhang, B., Wang, Y., Zhu, H., Huang, S., Zhang, J., Wu, X., et al., 2022. Evaluation of H_2S gas removal by a biotrickling filter: effect of oxygen dose on the performance and microbial communities. Process Saf Environ Prot 166, 30–40. https://doi.org/10.1016/j.psep.2022.07.054.